

博士論文

論文題目 Elucidation of physiological function of SCAP, a
crucial sterol-sensor molecule in astrocytes

(ステロールセンサー分子 SCAP のアストロ
サイトにおける生理的機能の解明)

氏名

周 聖浦

Table of Contents

	Pages
I. Abstract	3
II. Keywords	5
III. Abbreviations	6
IV. Introduction	9
V. Materials and Methods	17
VI. Results	33
VII. Discussion	43
VIII. Conflict of Interests	55
IX. Acknowledgement	56
X. References	57
XI. Figures	67

I. Abstract

Previous studies have proven that diabetic status combined with deficiency in insulin signaling leads to impairment of cholesterol synthesis in situ in the brain and decrease in content of total cholesterol in synaptosomal membrane. Dysfunctional regulation of cholesterol synthesis by sterol regulatory element-binding protein 2 (SREBP2) and SREBP-cleavage activating protein (SCAP) in the central nervous system has been proposed as one of the promising mechanisms linking diabetes mellitus and neurodegenerative disorders including cognitive dysfunction. However, little is known about the detailed roles of cholesterol synthesis regulators in cellular levels. Here we focused on cholesterol synthesis in glial fibrillary acidic protein (GFAP)-positive cells, mostly astrocytes, since they were essential for growth of neurons, stability of tripartite synapse, neurotransmitter homeostasis and maintenance of blood-brain-barrier integrity. We found that genomic SCAP knockout in primary culture astrocytes resulted in defects in cell proliferation, cellular growth, and survival in serum-free medium. Moreover, less anxiety, improper stress responses and impaired consolidation of long-term memory evaluated by correlational behavioral tests were noted in *hGFAP-CreERT2(Tg)::SCAP flox* mice in which SCAP knockout was inducible by intraperitoneal tamoxifen injections. There were no apparent structural abnormalities

in hippocampus and paraventricular regions. No differences in glucose tolerance, insulin sensitivity, food consumption, motor co-ordination or stress-related hormonal regulations were found. Although exact mechanisms are yet to be identified, tripartite synapse instability, dysfunctional blood-brain-barrier, variations in adult neurogenesis and inadequate inflammatory cytokine responses such as interleukin 6 might be the possible clues.

II. Keywords

diabetes mellitus; cognitive dysfunction; dementia; sterol regulatory element-binding protein (SREBP); SREBP-cleavage activating protein (SCAP); glial fibrillary acidic protein (GFAP); astrocytes ; immunopanning; adult neurogenesis

III. Abbreviations

4-OH tamoxifen: 4-hydroxytamoxifen

ACTH: adrenocorticotrophic hormone

ANG-1: angiotensin-1

APP: amyloid precursor protein

BBB: blood brain barrier

BPSD: behavioral and psychological symptoms of dementia

CoA: coenzyme A

CRH: corticotrophin-releasing hormone

CreERT2: Cre recombinase fused to a mutated ligand-binding domain of the human estrogen receptor

DM: diabetes mellitus

GFAP: glial fibrillary acidic protein

H&E staining: hematoxylin and eosin staining

HBEGF: heparin-binding epidermal growth factor

HMG CoA: hydroxymethylglutaryl-coenzyme A

HPA axis: hypothalamus-pituitary-adrenal gland axis

HS/DMEM: horse serum in Dulbecco's modified eagle medium

Hmgcr: hydroxymethylglutaryl-coenzyme A reductase

IL-6: interleukin 6

IL-6RA: interleukin 6 receptor alpha

i.p.: intraperitoneal (in tamoxifen administration)

IP: immunopanning (in primary astrocyte culture)

ITGB5: integrin beta 5

ITT: insulin tolerance test

Insig1: insulin induced gene 1

L1CAM: L1 cell adhesion molecule

Ldlr: low density lipoprotein receptor

MHLW: Ministry of Health, Labor, and Welfare

NADPH: nicotinamide adenine dinucleotide phosphate.

NORT: novel object recognition test

OGTT: oral glucose tolerance test

PLL: poly-L-lysine

SDS-PAGE: sodium dodecyl sulfate poly-acrylamide gel electrophoresis

SCAP: SREBP cleavage activating protein

SREBP: sterol regulatory element-binding protein (gene nomenclature as: Srebf)

STZ: streptozotocin

Sqle: squalene monooxygenase

Tam: tamoxifen

VEGF- α : vascular endothelial growth factor-alpha

WAT: white adipose tissue

WD: WD40 domain

bHLH: basic helix-loop-helix leucine zipper

IV. Introduction

Diabetes mellitus (DM), which is characterized by a status of pancreatic beta cells dysfunction, decreased insulin signaling and pathological elevated blood glucose level, has become much more common all over the world. Increased longevity which was ascribed to the medical advancement and effectiveness of infectious control combined with an affluent lifestyle also brought high prevalence of type 2 diabetes in the elderly as a serious healthcare burden among all developing and developed countries¹. According to the survey of Ministry of Health, Labor and Welfare (MHLW) in Japan in 2012, it was estimated that 11 million of people had impaired glucose tolerance and 9.5 million had diabetes. Among diabetic population, the ratio of the elderly has increased by year. In 2012, around 76 percent of diabetic patients were presumed to be older than 60 years old. Moreover, diabetes is also notorious for its complications. Without appropriate glycemic control, the risk of progression in microvascular complications such as neuropathy, retinopathy and nephropathy, as well as cerebral and cardiovascular morbidities, has been proven to increase significantly according to the evidences of several large clinical trials in the last two decades²⁻⁴. Understanding the detailed mechanisms by which poor glycemic control causes relevant complications is one of the most important topics nowadays.

With growing populations of elderly people, cognitive dysfunction and later-onset dementia gather much more attention than before in terms of not only medical but socio-economic problems. As a matter of fact, the progression of cognitive impairment and dementia is one of the serious diabetic complications. In 1999, Ott A, et al. reported a prospective population-based cohort study among elder subjects and demonstrated that DM nearly doubled the risk of dementia⁵. Moreover in Japan, Ohara T, et al. investigated the association between glucose tolerance and the progression of all types of dementia in the Hisayama study for a follow-up of 15 years and found that diabetes, especially post-load high glucose levels in oral glucose tolerance test, had statistically significant associations for all-cause dementia, Alzheimer's diseases and vascular dementia⁶. Later-on meta-analysis summarized the clinical evidences that hazard ratios in subjects with DM were around 1.6, 2.2 and 1.7 for Alzheimer's disease, vascular dementia and all-caused dementia, respectively compared with those without DM⁷. Nowadays several hypotheses had been proposed and it was generally believed that abnormal processing of amyloid beta, tau overphosphorylation, oxidative stress, formation of advanced glycation end products, and inflammation, as well as impaired cholesterol synthesis due to insufficient insulin action in the brain could be possible mechanisms to explain the close interaction between diabetes and dementia⁸. Further

studies are still warranted to elucidate the details.

Cholesterol is abundant in mammalian brains. It is estimated that 20-25% of the total amount of the cholesterol present in humans is localized in brains; approximately 70% of the brain cholesterol is present in myelin⁹. Moreover, because of isolation with blood brain barrier (BBB) and lack of identifiable carriers or efficient routes for lipoprotein transportation, cholesterol homeostasis in mammalian brains is well-known to be a highly closed environment and its excretion is nearly dependent on enzymatic conversion of cholesterol to 24-hydroxycholesterol, which is capable of passing through BBB¹⁰. As a result, cholesterol in the brain is generally insulated from circulating cholesterol and nearly 95% of the cholesterol in the brain was supposed to be in situ synthesized¹¹. In humans, disorders of cholesterol homeostasis in the brain cause neurological deficits and sometimes fatal. For example, Huntington's disease, which is famous for its neurodegenerative symptoms including unsteady gait and involuntary movements, dysphagia, progressive dementia, and seizures, is reported to have defects in cholesterol synthesis in central nervous system according to mouse models and autopsy data from humans¹². The Smith-Lemli-Opitz syndrome is caused by a mutation in the 7-dehydrocholesterol reductase gene, leading to accumulation of its direct precursor 7-dehydrocholesterol in the brain. Cerebellar ataxia, seizures and mental

retardation in the early stage are common features of this syndrome¹³. In addition, the genetic analysis of late-onset Alzheimer's disease has demonstrated that carrying certain subtype (epsilon 4) alleles of *APOE*, a major apolipoprotein involved with cholesterol metabolism in the brain, is an independent risk factor for its pathogenesis forming pathological amyloid plaques since early stage of the disease¹⁴.

Lipid biosynthesis is regulated under the control of sterol regulatory element-binding proteins (SREBPs) and SREBP-cleavage activating protein (SCAP). SREBPs are transcriptional factors responsible for expression of more than 30 genes involving synthesis and/or uptake of sterol, phospholipids and fatty acids (Fig. 1). Mammalian species have two predominant SREBP isoforms, SREBP1c and SREBP2; SREBP1c regulates genes required for fatty acid synthesis, whereas SREBP2 is responsible for cholesterol metabolism. SREBP precursors are located in the endoplasmic reticulum (ER) in association with SCAP. When intracellular sterol levels are low, SREBP2 precursor is transported to Golgi apparatus where the proteolytic processing for activation by two specific proteases occurs. Activated SREBP forms dimer and directly binds to SRE (sterol regulatory element) in the enhancer/promoter region of target genes (Fig. 2)¹⁵. Both SREBP1c and SREBP2 genes share SRE in their enhancer/promoter regions, indicating that mature SREBPs also upregulate transcription of themselves by

feed-forward regulation^{16, 17}. Transportation of SREBPs from ER to the Golgi apparatus requires SCAP, an escort membrane protein responsible for function of sterol-sensing and stabilization of SREBPs in ER. Previous studies showed that hepatocytes lacking SCAP have low levels of mature form of both SREBP1c and SREBP2 with decreases in mRNA expression of related biosynthetic enzymes¹⁸.

The mechanisms of defective cholesterol synthesis in brains connecting diabetes and neurodegenerative diseases have been under investigations. Suzuki et al. previously reported that mRNA expressions of SREBP2 and its downstream genes were significantly downregulated in the mouse hypothalamus and cortex with insulin-deficient diabetes induced by injection of streptozotocin (STZ)^{15, 19}. Total amount of cholesterol content in the synaptosomal membrane extracted from the brain was also found to be decreased. Furthermore, intracerebroventricular administration of insulin reversed this downregulation, whereas normalization of blood glucose levels by administration of phlorizin did not, demonstrating that impaired insulin action, rather than high glucose levels, was responsible for this alteration. In vitro knockdown of SREBP2 by shRNA lentivirus in isolated neurons revealed a decrease in markers of synapse formation¹⁹. Successive experiments showed that in brains of diabetic mice, the amount of SCAP protein decreased. Homozygous knockout of *Scap* in the central

nervous system by the Cre-loxP system using nestin-Cre transgenic mice and *Scap* floxed mice caused perinatal lethality associated with microcephaly. Adult heterozygous *Scap* knockout mice with the nestin-Cre showed a decrease in cholesterol synthesis in the brain by 30 percent, which was similar to that in diabetic mice²⁰. Impairment in synapse function in the hippocampus and recognition memory was noted in this mouse model evidenced by neural electrophysiological studies and behavioral tests such as novel object recognition test²⁰. Therefore, as a possible mechanism for diabetes-induced dementia and other neurodegenerative diseases, it is hypothesized that severe hyperglycemia and impaired insulin action disturb the homeostasis of cholesterol metabolism in the brain via lowering expression of SCAP, SREBP2 and its downstream sterol-producing genes. Disturbed cholesterol metabolism in the central nervous system is believed to cause hypoplasia of synapses, and defected synaptic transmission, both of which may lead to impaired cognitive function and abnormalities in stress response (Fig. 3). However, detailed phenotypes and mechanisms by which cholesterol insufficiency causes in individual cell types or in certain areas of brain still remain unanswered. In addition, postnatal significance of the regulation of SREBP/SCAP system for brain function is less understood.

Both neurons and astrocytes are capable of synthesizing cholesterol. Neurons in

adulthood are responsible for signal transmission by induction of action potentials and release of neurotransmitter via synapses as a core part in central nervous system, while astrocytes act more like supporters of neurons by defining the brain microarchitecture, providing neurons with metabolic resources, maintaining glutamatergic neurotransmission, controlling extracellular potassium homeostasis and regulating neurite outgrowth and synaptogenesis²¹⁻²³. Therefore, it is reasonable to assume that astrocytes are critical for maintaining cholesterol homeostasis in the brain with a high capacity during adulthood compared with neurons. Glial fibrillary acidic protein (GFAP), which is expressed mainly in astrocytes, is a representative astrocyte-specific marker. Conditional knockout of *Scap* in the astrocytes, represented by GFAP-positive cells in this study, is a suitable model to evaluate the cell type-specific importance of sterol metabolism in the central nervous system.

Another point in this study lies on the timing of gene expression. Cognitive impairment in diabetes is not supposed to be congenital but is generally considered to be the defects after birth. Our previous study used a mouse model with nestin-Cre showing disorder in lipid metabolism in the brain since early developmental stages²⁰. Therefore, the potential influences of developmental abnormalities in the embryonic stage could not be totally ruled out. In order to explore the impact of cholesterol

homeostasis linking diabetes and neurodegenerative diseases, we employed a conditional knockout model by an inducible manner to circumvent this problem.

The objectives of this study were to clarify the role of SCAP in GFAP-positive astrocytes by using an inducible approach to knockout SCAP expression in vitro and in vivo. We studied the impact of SCAP deficiency in primacy culture astrocytes, and examined phenotypes of a mouse model with inducible *Scap* knockout in the astrocytes, in order to elucidate the mechanisms and find clues for possible treatment of cognitive impairment in diabetes or other neurodegenerative diseases in the future.

V. Materials and Methods

Animals and primers for genotyping

Mice were housed in a temperature- and light-controlled environment maintaining the animal's diurnal cycle (12 h light and 12 h dark) with an ad libitum standard mouse chow. All procedures were approved by the faculty's animal experimentation committee.

The hGFAP-CreERT2 transgenic mice were kindly provided by Dr. Frank Kirchhoff (Germany). The hGFAP-CreERT2 transgene was constructed and contained the human *GFAP* promoter, a tripartite intron, the open reading frame of CreERT2 and the human growth hormone poly A site as the same as previous studies^{24,25}. We mated the mice with *Scap* flox mice purchased from the Jackson Laboratory (USA) via CLEA, Japan. In the mice, two loxP sites were inserted into the both side of *Scap* exon 1, identified as the flox allele. After mating repeatedly, we were successful to obtain the *hGFAP-CreERT2(Tg)::Scap flox* mice finally. In this model, tamoxifen administration by intraperitoneal (i.p.) injection was supposed to lead to genomic recombination of *Scap* gene by tamoxifen-inducible activation of Cre recombinase to inactivate the expression of SCAP transcriptionally in GFAP-positive cells, mostly astrocytes in the central nervous system. The genomic recombinant mice lacking SCAP were believed to decrease cholesterol synthesis in the target cells according to previous studies¹⁸.

We designed the primers to confirm successful genomic recombination by DNA genotyping. The details are as follows:

SCAP forward: 5' - GCT CTG CGC ATC CTA TCC AAT TCC C-3'

SCAP reverse: 5' - CAG CCG GCA AGT AAC AAG GGA TCC G-3'

SCAP delta forward: 5' -GCC TTT CTG GAA CTT GCT CTG TTG G- 3'

Cre forward: 5' - CCT GGA AAA TGC TTC TGT CCG- 3'

Cre reverse: 5' -CAG GGT GTT ATA AGC AAT CCC-3'

We used the genome extracted from liver samples of *Scap* flox/flox mice after intravenous injection of adeno-Cre vector as a positive control of loxP recombination, and the genome from C57Bl/6J mouse tails as a wild-type control (Fig. 4). All mice used for experiments except primary cell culture were male.

Primary culture

Classical astroglial cell culture

This widely employed method was described previously²⁶. In brief, dissected cortices from P0-P1 *hGFAP-CreERT2(Tg)::Scap flox* mice were gathered after euthanasia on ice. Genotyping of Cre was confirmed and separated initially before sorting. Trypsin treatment followed by addition of trypsin inhibitor and gentle trituration was performed

to yield suspension of single cell mixture. Then cells were suspended in 10% horse serum in HS/DMEM on PLL-coated plastic wells. In Cre-positive groups, 4-OH tamoxifen (4-hydroxytamoxifen, 1 μ M) was applied to activate genome recombination. RNA was extracted after 80% confluent was achieved by light microscopy.

Immunopanning purification of primary astrocytes

To harvest more highly purified GFAP positive cells, we also performed primary culture of astrocytes by method of immunopanning, which was initially published²⁷ in 2011, with slight modifications. We used non-specific IgG (Jackson) and antibodies against CD45 (BD Bioscience), oligodendrocyte marker 4 (O4) (R&D Systems), and L1 cell adhesion molecule (L1CAM) (Millipore) to remove macrophages, microglia, oligodendrocytes and neurons from cell mixture suspension in the beginning. We also used an antibody against integrin beta 5 (ITGB5), a surface marker expressed exclusively in astrocytes, to positively select astrocytes (R&D Systems) and washed out the remaining tissue debris finally. Medium for astrocyte growth did not contain serum but addition of heparin-binding epidermal growth factors (HBEGF) (Sigma-Aldrich) was necessary as growth factors. In Cre-positive groups, 4-OH tamoxifen (100 nM) was applied to activate genome recombination. The procedure is summarized in Figure 5.

Behavioral experiments

We performed tamoxifen i.p. administration when the *hGFAP-CreERT2(Tg)::Scap flox* mice were eight to nine weeks of age. Two milligrams of tamoxifen (dissolved in 10% Ethanol/ sunflower oil) were injected once per day for consecutive 8 days. Then we performed all behavioral tests from 9 to 16 weeks of age as a battery. The sequence of the experiments was listed as follows: elevated open-platform test at 9-10 weeks of age; Y maze at 10 weeks of age; novelty suppressed feeding at 10-11 weeks of age; novel object recognition test at 11 weeks of age; rotarod at 11-12 weeks of age; tail suspension test at 12-13 weeks of age; social recognition test at 13-14 weeks of age; forced swim test at 13-15 weeks of age; elevated plus maze test at 14-15 weeks of age; passive avoidance test at 14-16 weeks of age. Experiments including fasting (e.g. novelty suppressed feeding) and pain (e.g. passive avoidance test) were performed at the last of the battery or independently.

Elevated open-platform test

This test was performed to evaluate psychological stress, as described previously²⁸. A transparent acrylic cylinder (11.4cm in diameter, 18cm in height) was placed upside-down and each mouse was positioned at the top as open platform in order. Then we counted the duration of freezing in 8 minutes. If the mouse in trial was slipped off the platform,

the mouse was immediately placed back on the platform and the experiment was continued.

Novelty suppressed feeding

This test was performed to evaluate depressive status, anxiety, and fear, as described previously²⁹. After 24 hour fasting in the home cage, the test mouse was placed in the corner of the box with regular bedding. In the middle of the box, a metal round plate with a hole in the center was placed and two pellets of food (regular chow) were put on the hole. The video was recorded for 6 minutes for each mouse. The latency and duration of entering the metal plate ("arena") and finally chewing the pallet was calculated. This setting induces a conflicting motivation between the drive to eat the food pallet by hunger and the fear of venturing into the unfamiliar metal plate.

Elevated plus maze test

This test is well-known for evaluation of anxiety-related behavior³⁰. Briefly, a mouse was placed at the junction of the four arms of the elevated maze (Shin factory) consisting of two closed arms with surrounding walls and two open arms without surrounding walls. Entries and duration in close and open arms were recorded by a video-tracking system and observer simultaneously for 500 seconds. An increase in open arm activity (both duration and entries) reflected less anxiety behavior. Time was

not counted when the mouse stayed in the junction of the maze.

Tail suspension test

This test was first described in 1985 by Steru L. as a method for screening antidepressants in the beginning, and became a useful tool to assess depressive status in mice³¹. The mouse in trial was elevated at least 25 cm from the floor by being suspended by the tail with tape on the acrylic box. Each mouse was given one trial that lasts 6 minutes. All movements were recorded by a video camera. The latency and total duration of immobility, defined as the absence of initiated movements, including passive swaying, were calculated. The longer the duration, the higher risk of desperate status the mouse had.

Forced swim test

In common with the tail suspension test, this test is widely used for evaluation of antidepressant drugs and assessment of depressive-like states. We used the protocols of previous studies as references³². Mice were forced to swim in a transparent cylinder (19 cm in diameter with water of 19 cm in depth) from which they could not escape. We tested two mice simultaneously in adjacent cylinders separated by an opaque plate. The test lasted for 6 minutes. We scored duration and latency of immobility during the last 4 min of the 6-min test session. Immobile was defined as the time not spent actively

exploring the cylinder or trying to escape from it. Short periods with small movement which was necessary to maintain their heads above water were counted as immobile.

Y maze

This test is generally used for measuring the willingness of mice to explore new environments and evaluations for hippocampal-dependent working memory³³. The mouse was placed in the corner of one arm of the arena which had three arms and was shaped like 'Y' (Shin factory). Movement of the mouse was recorded for 8 minutes. The number of arm entries and the arm number of triads were recorded in order to calculate the percentage of alternation. An entry was defined as a state when all the four limbs were within one arm.

Novel object recognition test (NORT)

We performed this test as described previously with slight modifications²⁰. This test took 6 days to accomplish. From day 1 to day 4, handling the test mouse for 6 minutes, followed by placing it in the arena without bedding for additional 6 minutes, was required for environment habituation. The arena was made of acryl, grey in color and 40, 40, 45 cm in length, width and height, respectively. At day 5, two identical objects (cubes, 4 cm on a side) were placed in the diagonal corner of the arena, the activity and movement were recorded by a video for 15 minutes. Total time of touching and sniffing

(defined as less than 1cm distance from the nose of mouse to the object) was calculated.

At day 6, we repeated the same 15-minute observation but this time one of the cubes was replaced by a ball (4 cm in diameter) with the same material. The time when the mouse stood on the object was excluded. This test is useful in providing an index of recognition memory³⁴.

Social recognition test

The details of this test were already described in previous studies³⁵. This test probes recognition and working memory, providing a relatively high sensitivity to investigate novel target mechanisms relevant to cognitive impairment associated with neuropsychiatric disorders such as Alzheimer's disease (AD). In brief, each test mouse was placed in a cage for one hour, then a BALB/c mouse (4 weeks of age) was placed inside as an intruder. We observed the interactions for 90 seconds. The test mouse and the BALB/c mouse were pair-labeled in advance. Total duration when the test mouse approached the BALB/c mouse was summed. The session of interaction finished after 90 seconds and the BALB/c mouse was removed from the cage. After 2 hours and 24 hours, we repeated the second and the third sessions again and saw if the total time of interaction changed with time.

Passive avoidance test

This test is a trial of fear-motivated avoidance task for evaluation of long term memory. The detail was described previously³⁵. In brief, a mouse was at first placed in the light room of an apparatus, which was composed of a light room and a nearby dark room with a door closed (O'Hara & Co., Ltd.). After the door was open by manual, the time was recorded when the mouse entered into the dark instinctively. When all the four limbs of the mouse were in the dark room, an episode of mild and unharmed electrical shock was given (0.2 mA for continuous 2 seconds). The mouse was immediately removed from the apparatus and returned to its home cage. Twenty-four hours later, we performed the second trial without giving electrical shocks anymore. The third trial was practiced again after one month. The latency to enter the dark room was served as an index of assessment for long term memory.

Rotarod

This test is used to evaluate motor co-ordination, balance and motor learning of mice³⁶. The mouse was placed on the rod of the apparatus (Med Associates, Inc.) firstly in a very slow rotation speed without difficulties, then the rotation rate of the rod was accelerated gradually over the course of the test session (4 to 40 rpm in 5 minutes). Once the mouse falling off from the rod, the time was recorded and the trial finished. We performed 6 trials in a 90-minute interval for each mouse to assess the motor

learning skill in the same day. If the mouse stood on the rod for more than 6 minutes, then 6 minutes was determined.

OGTT (oral glucose tolerance test) and ITT (insulin tolerance test)

These two procedures were performed as described previously^{37, 38}. For OGTT, the mice were fasted for 12-16 hours, and the blood samples were obtained at the indicated time points after the oral administration of 2 g/kg body weight of D-glucose (WAKO).

For insulin tolerance test (ITT), the mice were fasted for 12-16 hours, and the blood samples were obtained at the indicated time points from tail after the i.p. injection of human regular insulin (1 U/kg body weight, Lilly). Blood glucose levels were checked at indicated time points (Glutest Pro; Sanwa Kagaku Kenkyusho).

Stress-related hormone measurements

All the protocols were modified from the previous study³⁹. We collected blood samples from facial vein of the mice at 9 AM and 9 PM on the same day, and at 9 AM again after a 12-hour fasting period two weeks later. Stress-related hormones (epinephrine, corticosterone, adrenocorticotrophic hormone (ACTH) and corticotropin-releasing hormone (CRH)) were measured by mouse epinephrine,

corticosterone, ACTH ELISA kits (CUSABIO) and the mouse CRH ELISA kit (USCN).

In addition, we restrained the mice on a plastic plate individually for continuous 40 minutes and collected blood samples before, soon after, 30 and 120 minutes after the restraint. Serum corticosterone levels were measured. The procedure of sample measurement was followed by kit instructions.

Quantitative RT-PCR

We isolated total RNA from fresh-frozen tissue of different areas of the brain or cultured cells by using the RNeasy Universal Kit (Qiagen). After measuring the yields of RNA, we synthesized cDNA by using High-Capacity cDNA Reverse Transcription Kit (Applied Biosystems). Finally quantitative real-time PCR was performed with PCR Master Mix reagent and ABI Prism 7900HT sequence detection system (Applied Biosystems). All procedures were performed under the standard instructions. Beta-tubulin and TATA box binding protein (TBP) were used as internal controls.

The sequences of the primers and probes used for detection of cholesterol synthesis gene expression were as follows:

Beta actin: Mm00607939-S1 (Invitrogen®)

TBP forward: 5'-ACC CTT CAC CAA TGA CTC CTA TG-3'

TBP reverse: 5'-TGA CTG CAG CAA ATC GCT TGG-3'

SCAP forward: 5'- ATG ACC CTG ACT GAA AGG CTT CGT- 3'

SCAP reverse: 5'- TAA CCC TTC ACA GGC GTG GAG AAT- 3'

Cre forward: 5'- CCT GGA AAA TGC TTC TGT CCG- 3'

Cre reverse: 5'-CAG GGT GTT ATA AGC AAT CCC-3'

Srebf1a forward: 5'-GGC CGA GAT GTG CGA ACT -3'

Srebf1a reversed: 5'-TTG TTG ATG AGC TGG AGC ATG T-3'

Srebf1c forward: 5'-GAG CCA TGG ATT GCA CAT TT-3'

Srebf1c reversed: 5'-CTC AGG AGA GTT GGC ACC TG-3'

Srebf2: Mm01306292-m1 (Invitrogen®)

Hmgcr forward: 5'-TCA GTG GGA ACT ATT GCA CCG ACA-3'

Hmgcr reverse: 5'-TGG AAT GAC GGC TTC ACA AAC CAC-3'

Ldlr forward: 5'-CAA CAA TGG TGG CTG TTC CCA CAT-3'

Ldlr reverse: 5'-ACT CAC ACT TGT AGC TGC CTT CCA-3'

Sqle forward: 5'-TTG TTG CGG ATG GAC TCT TCT CCA-3'

Sqle reverse: 5'-GTT GAC CAG AAC AAG CTC CGC AAA-3'

Insig1 forward: 5'-TCA CAG TGA CTG AGC TTC AGC A-3'

Insig1 reverse: 5'-TCA TCT TCA TCA CAC CCA GGA C-3'

Gfap forward: 5'-TCA ACG TTA AGC TAG CCC TGG ACA-3'

Gfap reverse: 5'-TCT GTA CAG GAA TGG TGA TGC GGT-3'

IL-6 forward: 5'-GCT TAA TTA CAC ATG TTC TCT GGG AAA -3'

IL-6 reverse: 5'-CAA GTG CAT CAT CGT TGT TCA TAC -3'

IL-6 receptor alpha: Mm00439653-m1 (Invitrogen®)

VEGF- α forward: 5'-CCT GGT GGA CAT CTT CCA GGA GTA CC-3'

VEGF- α reverse: 5'-GAA GCT CAT CTC TCC TAT GTG CTG GC-3'

ANG-1 forward: 5'-GAA GGG AAC CGA GCC TAC TC-3'

ANG-1 reverse: 5'-GAG CGC ATT TGC ACA TAC AG-3'

Immunoblotting

Immunoblotting was conducted as previously described³⁷. In brief, cytoplasmic protein extracts from cell cultures were obtained by NE-PER Reagents (Thermo Fisher Scientific Inc). Then protein was separated by SDS-PAGE and electroblotted 2 hours onto poly-vinylidene difluoride membranes. Membranes were probed with the primary antibodies against anti-beta actin antibody (1:5000, Sigma-Aldrich) or anti-SCAP antibody (1:200, Santa Cruz SC9675) overnight. Secondary antibodies (anti-goat IgG-HRP (Santa Cruz SC2056) and anti-rabbit IgG-HRP (1:6000, GE NA934V) were

used in the next day. We used the Enhanced Chemiluminescence (ECL) Western Blotting Detection System Kit™ (Amersham) for Western blot detection of immunoblotted proteins. Finally membranes were scanned with a luminescent image analyzer (LAS-4000, Fujifilm). Quantification was performed by using Image J software.

Immunostaining

Cultured cells were stained under the protocol of previous studies⁴⁰. At first, cells were fixed with 4% paraformaldehyde in phosphate buffered saline (PBS) for 20 minutes. We permeabilized the cells by 0.1% Triton X in PBS for 10 minutes three times. Later cells were incubated with primary antibodies (mouse anti-GFAP (1:400, Millipore MAB360); rabbit anti-beta tubulin (1:100, Cell Signaling 2146S)) in four degrees of Celsius overnight. After wash by 0.1% Triton X in PBS three times, conjugated secondary antibody (anti-mouse-Alexa 568 (1:1000, Molecular Probes A11031) and anti-rabbit-Alexa 488 (1:1000, Molecular Probes A11034)) was incubated for 60 minutes under room temperature. Nuclear staining was performed by Hoechst (Sigma B2261). Digital images were obtained with compatible software using the epifluorescence microscope (FSX-100, Olympus).

The protocol of immunostaining in brain tissues was similar to that in cell cultures, but we selected different GFAP primary antibody (rabbit anti-GFAP (no dilution, DAKO IS52430) for high image resolution of immunostaining.

Preparation of brain slices and hematoxylin and eosin staining

After euthanasia by i.p. injection of mixture of medetomidine, midazolam and butorphanol tartrate, male mice aged 10-12 weeks were perfused by 4% paraformaldehyde. After that, the whole brain was extracted and fixed in 4% paraformaldehyde at 4 degrees of Celsius for 48 hours. Two days later, the fixed whole brain was coronally dissected into three parts: anterior, middle and posterior, dehydrated serially by different concentration of ethanol and xylene, finally embedded in paraffin blocks. Six micrometer thick coronal sections were performed for histological analysis. Hippocampus, dentate gyrus and paraventricular regions were of particular interest in this study. We selected and determined the sections according to the atlas of mouse brain (Paxinos and Franklin's The Mouse Brain, Fourth edition).

Standard hematoxylin and eosin staining (H&E staining) was performed to evaluate the structural variations in hippocampus and periventricular regions.

Statistical Analysis

Data were presented as group mean \pm SEM. We performed statistical comparisons between two groups by an unpaired Student's t-test (parametric) or Mann-Whitney U-test (non-parametric) for most of results. For passive avoidance test and rotarod, an analysis of Friedman's X^2 r-test was performed; if the statistical significance was reached, then we performed Wilcoxon t-test with Bonferroni correction as post hoc test. $P < 0.05$ or less was considered statistically significant in this report.

VI. Results

Generation of hGFAP-CreERT2(Tg)::Scap flox mice

By intercrossing *hGFAP-CreERT2(Tg)* mice with *Scap* flox/flox mice, we obtained a new strain of *hGFAP-CreERT2(Tg)::Scap flox* in our laboratory. According to the design of primers, *Scap* flox band should be intact no matter Cre recombinase existed or not in genome if tamoxifen was not given. After i.p. administration of tamoxifen, the *Scap* gene in GFAP positive cells was supposed to be partially deleted and knockout bands would appear by DNA genotyping in the whole brain where astrocytes resided. We confirmed the knockout bands in thalamus, hypothalamus, cortex and cerebellum of Cre positive mice after tamoxifen administration (Fig. 7A). In addition, these knockout bands existed at 45 weeks of age after tamoxifen induction at 8 weeks of age (Fig. 7B). No knockout bands were detected in Cre positive mice if no tamoxifen was given, and were detected either in liver, heart, skeletal muscle or white adipose tissue after tamoxifen administration, as our expectations (Fig. 7C). In conclusion, we confirmed that this animal model worked and was useful for our study.

Some concerns about disturbance in growth may be raised due to tamoxifen toxicity or insertion of Cre-loxP system in the central nervous system. Previous reports demonstrated that mice carrying the nestin-Cre transgene exhibit a marked metabolic

phenotype as lower body mass and a significant reduction in brain size and body length⁴¹. On our animals, there were no significant differences in body weight changes between Cre positive and negative mice before and after tamoxifen administration from 5 to 20 weeks of age. Total dose of tamoxifen given in our study did not alter significant changes in body weight, ruling out its toxicity to influence growth and survival (Fig. 8A). Brain slices revealed that no enlargement of ventricles, apparent atrophy or other anatomical abnormalities in the hippocampus and paraventricular regions were noted by H&E staining between Cre positive and negative mice after administration of tamoxifen (Fig. 8B). Genomic recombination of *Scap* in astrocytes did not cause obvious differences in numbers of GFAP-positive cells in areas of hippocampus evidenced by immunostaining of brain tissue (Fig. 8C).

Decreased expression of Scap mRNA and SCAP protein levels and its downstream related genes in primary Cre positive astroglial cultures after tamoxifen induction

Next we tried to confirm the reduction of SCAP expression in GFAP positive cells after tamoxifen induction. We could not identify any differences in transcriptional levels of *Scap* expression from brain tissue between *hGFAP-CreERT2(Tg)::Scap flox* mice with and without tamoxifen administration presumably because not only astrocytes

but also the other cell types e.g. neurons, oligodendrocytes, microglials, or endothelial cells also expressed *Scap* to mask the reduction (Fig. 9).

To overcome this problem, we performed primary astrocyte-rich cell culture from P0-P1 brains of *hGFAP-CreERT2(Tg)::Scap flox* mice. We sorted the brain samples according to the existence of Cre recombinase by DNA genotype initially. It was shown that *Scap* expression in RNA and SCAP protein levels were significantly reduced to around 40 percent in Cre positive primary astroglial culture by quantitative rt-PCR and western blotting, respectively, after 4-OH tamoxifen was given, while no changes in *Scap* expression were found in Cre-negative primary culture (Fig. 10A and 10B). Significant downregulation of *Srebf2* and *Srebf1c* in the cells suggested that cholesterol and fatty acid synthesis might be suppressed. Although no changes in expression of *Srebf1a* could be identified, decreased expression of cholesterol-synthetic enzymes such as *Hmgcr* and *Sqle* in transcriptional level was found in Cre positive cultures after induction (Fig. 10C). No changes were shown in Cre negative cultures under tamoxifen induction of the same concentration (data not shown). Increased concentration of 4-OH tamoxifen (up to 30 μ M) did not result in better efficiency of SCAP inhibition in transcriptional and translational levels (data not shown).

SCAP was an important factor in growth and survival for primary astrocyte culture by the method of immunopanning in vitro

Although expression of SCAP was decreased to around 40%, we did not observe any other morphologic changes in traditional primary astroglial culture. There were several possible reasons to explain the result: firstly, the procedure of traditional astroglial culture was convenient and straightforward, but most of growing astroglial cells, different from those in vivo, were fibroblast-like and lacking delicate perisynaptic astrocyte processes, as reported by previous studies⁴². Secondly, some progenitor cells and glial cells other than astrocytes would not be ruled out in the traditional primary culture. Furthermore, in spite of impairment in cholesterol de novo synthesis due to SCAP deficiency, astrocytes might be able to uptake cholesterol directly from the serum-containing medium in which cholesterol-rich lipoprotein was abundant. To overcome these problems, we decided to perform another primary astrocyte culture more physiological with higher purification as the method of immunopanning, which was first described by Foo et al. in 2011²⁷. By their method, a defined, serum-free medium was available for purified astrocytes to survive in long-term culture.

Compared with traditional primary astroglial culture, astrocytes purified by the method of immunopanning revealed that these cells had more process-like structures,

and the ratio of GFAP-positive cells dramatically increased (Fig. 11). Besides, the number of surviving cells decreased significantly in Cre positive cell culture after 4-OH tamoxifen addition by light microscopy in the method of immunopanning (Fig. 12A). No such differences could be observed in traditional primary culture. The *Scap* mRNA expression and SCAP protein levels were also dropped around 40% in the method of immunopanning, similar to those in traditional primary culture. Profiles of other related genes involved in cholesterol synthesis and uptake were similar to the results of traditional astroglial culture, as expression of *Srebf2*, *Hmgcr*, *Ldlr*, *Sqle* and *Insig1* in transcriptional level was inhibited when *Scap* was conditionally knocked out by tamoxifen (Fig. 12B).

By immunostaining of GFAP, we found that the ratio of GFAP-positive surviving cells decreased significantly in Cre positive culture after tamoxifen induction. In transcriptional level, *Gfap* expression was also decreased in Cre positive cultures with tamoxifen compared to those without addition of 4-OH tamoxifen (Fig. 12C). No alterations of *Scap* and *Gfap* in transcriptional levels were found in Cre negative cultures no matter if 4-OH tamoxifen was given or not. All the above findings implied that *Scap* knockout led to a fatal defect presumably due to impaired cholesterol de novo synthesis. In addition, in serum-free medium, GFAP positive astrocytes could not extend

their growth and maintain survival if *Scap* was knockout by 4-OH tamoxifen. Decreased growth and survival of astrocytes could not attribute to the toxicity of 4-OH tamoxifen.

We also evaluated the effects of 4-OH tamoxifen concentrations. Apparent cell necrotic changes were observed when 1 μ M or higher concentration of 4-OH tamoxifen was given by the method of immunopanning (data not shown).

No significant changes of expression of interleukin 6 (IL-6), IL-6 receptor alpha (IL-6RA), VEGF- α and ANG-1 in both the traditional primary astroglial culture and the immunopanning astrocytes culture. (Fig. 13A and 13B)

Improper stress responses and impulsiveness were noted in GFAP-SCAP(-) mice

After administration of tamoxifen at 8 weeks of age, we performed several behavioral tests to determine the possible roles of SCAP in astrocytes in vivo. In elevated open platform test, *hGFAP-CreERT2(Tg)::Scap flox* mice after tamoxifen injection (represented as GFAP-SCAP(-) in the following for abbreviations) showed less time of freezing behavior when standing on the transparent narrow cylinder compared with *hGFAP-CreERT2(-)::Scap flox* mice after tamoxifen injection (represented as the control group in the following for easy-reading). Mice with the same weeks of age without tamoxifen injection did not show differences in total time of freezing between

two groups (Fig. 14A). Because elevated open platform test was used for evaluation of psychological stress, we performed similar stress-related tests such as novelty suppressed feeding and elevated plus maze test. In the elevated plus maze test, GFAP-SCAP(-) mice also showed more exploration of open arms (suggesting less anxiety) significantly than the control mice. The ratio of entering open arms over total time in arms was also significantly increased in GFAP-SCAP(-) mice (Fig. 14C). In the test of novelty suppressed feeding, although no statistical significance was reached, GFAP-SCAP(-) mice spent less time to enter the unfamiliar metal plate arena to start eating. The ratio of eating time during staying time in the arena was increased in GFAP-SCAP(-) mice (Fig. 14B). All the results above demonstrated that GFAP-SCAP(-) mice might show more impulsiveness under stress and make improper behavioral responses compared to the control mice.

To rule out the possibility that GFAP-SCAP(-) mice might potentiate the drive of hunger and result in less time to start eating in the test of novelty suppressed feeding, we counted on amounts of food intake for continuous three days after 24-hour-fasting. The result presented that no differences in food intake between the two groups in acute phase (first 3 hours) and in ordinary condition (after 3 hours). No differences in body weight changes were noted, either. Two groups did not show difference in food intake during

either light cycle or dark cycle (Fig. 14D).

Other than anxiety and fear, depressive state may also affect the results of stress-related behavioral tests. Tail suspension test and forced swim test are trustable tools to evaluate depressive state for rats and mice⁴³. No significant discrimination could be made between GFAP-SCAP(-) mice and the control mice in either tail suspension test or forced swim test, indicating that depressive condition would not be the core reason in interpretation of improper stress responses (Fig. 15).

Impaired consolidation of long term memory and social interaction were seen in GFAP-SCAP(-) mice but not short term memory and new object learning

Several behavioral experiments to test social interaction, reference memory, working memory and spatial learning were performed. It was found that GFAP-SCAP(-) mice had impairment in social interaction and recognition according to the results of the social recognition test. Gradual decrement of exploration time was noted in the control mice toward the same invader as the second and third contact, GFAP-SCAP(-) mice did not show this tendency and spent unchanged exploration time since the beginning (Fig. 16A). Moreover, defects in consolidation of remote memory was suggested in GFAP-SCAP(-) mice according to the results of passive avoidance tests. After only one

episode of mild electric shock (0.2mA for 2 seconds) that the mice had never experienced, both groups became hesitant to enter the dark chamber where they received the shock 24 hours ago. However, compared with the control mice, GFAP-SCAP (-) mice spent less latency to enter the dark chamber again when the same experiment was re-tested one month later, suggesting that establishment of long-term memory might be incomplete (Fig. 16B). Both groups of mice showed good performance in working memory and spatial learning in Y maze; both groups of mice showed interests to the novel object compared with the identical object in the novel object recognition test. Gathering all the results, it was indicated that genetic knockout of *Scap* in GFAP positive cells might not involve with difficulties in short-term memory and new object learning in a short period of time (Fig. 16C and 16D).

No differences in balance, motor learning, glucose tolerance, insulin sensitivity and stress-related hormones between GFAP-SCAP(-) mice and the control mice

Motor coordination can be affected by impairment in astrocytes because the cerebellum also contains numerous GFAP-positive Bergman glial cells. However, induction of *Scap* knockout in GFAP positive astrocytes did not result in worsening of balance, motor learning as evidenced by the results of rotarod (Fig. 17A).

GFAP-SCAP(-) mice even showed better running ability in the fourth trial compared with the control mice. Both groups showed significantly improved co-ordination and running ability since the third trial compared with the first trial. In addition, we did not find any differences between both groups in insulin sensitivity and glucose tolerance, as the outcomes of insulin tolerance test (ITT) and oral glucose tolerance test (OGTT) were similar without statistical significance (Fig. 17B).

Improper behavior responses under stress may be due to changes in stress-related hormones regulating by hypothalamus-pituitary-adrenal (HPA) axis according to previous studies⁴⁴. To evaluate this possibility, we checked diurnal rhythm of serum corticosterone, epinephrine, corticotropin releasing hormone (CRH) and adrenocorticotrophic hormone (ACTH) in the early morning (9 AM) and before night (9 PM) in both groups. Furthermore, we also evaluate the patterns of stress-related hormonal responses after the 12-hour-fasting in the dark cycle (as a chronic stressor) and after the 40-minute-restraint (as an acute stressor), however, no statistical differences could be detected regarding hormonal regulations (Fig. 18A-18C).

VII. Discussion

Lipid metabolism is highly conserved and delicately regulated in the mammalian cells. Insufficiency of insulin action in mammalian causes not only diabetes mellitus but also various metabolic disorders, including the cognitive impairment and mood disorders in the central nervous system⁴⁵. Previous studies already showed that severe hyperglycemic state combined with impaired insulin action was responsible for decrement of in situ synthesis of cholesterol in the central nervous system, however, the detailed effects of impairment in sterol synthesis in specific cells or brain areas were yet to be elucidated¹⁹. To understand the sterol regulations in the brain, we generated the transgenic mouse line of *hGFAP-CreERT2(Tg)::Scap flox* to study the roles of SCAP in GFAP positive cells, mostly astrocytes, for the ideas that sterol metabolism in the astrocytes were of importance in glia-neuron interactions and maintenance of micro-environment homeostasis. In this study, we found that reduction of SCAP, a crucial sterol-sensor molecule, downregulated both SREBP2 and SREBP1c, and their downstream genes in astrocytes. In addition, according to the results of primary astrocyte culture by method of immunopanning, we revealed that SCAP might play an important role for cellular survival and growth. Moreover, mice with inducible knockout of *Scap* expression in GFAP positive cells showed impairment in long-term memory and

improper stress responses evidenced by correlative behavioral examinations.

After tamoxifen administration, partially genetic recombination of *Scap* was confirmed by DNA genotyping in cerebrum, thalamus, hypothalamus, and cerebellum but not in organs other than brain in *hGFAP-CreERT2(Tg)::Scap flox* mice. Moreover, once tamoxifen was given at 8 weeks of age, the evidence of *Scap* recombination sustained for more than 9 months (42 weeks of age), indicating that recombination of *Scap* gene was not a temporary effect. To further prove the creditability of our mouse line, we focused on astroglial cells and performed primary cell culture by traditional method from P0-P2 *hGFAP-CreERT2(Tg)::Scap flox* mice, then added 1 μ M of 4-OH tamoxifen in the culture plate. Under this concentration of 4-OH tamoxifen, no influences on mRNA and protein expression of SCAP were noted in Cre negative culture but more than 40 percent decreases in *Scap* mRNA and SCAP protein were confirmed by rt-PCR and western blotting, respectively. Because the function of SCAP is to escort SREBPs from ER to the Golgi apparatus, deletion of *Scap* gene leads to inactivation of SREBPs, downregulating the expression of cholesterol-synthetic enzymes and SREBPs which had SRE in their promoter regions⁴⁶. Therefore, we also checked the expression of downstream genes regulating sterol and fatty acid synthesis, and found that recombination of *Scap* gene resulted in decreased expression of *Srebf2*,

Srebf1c and their downstream genes. All the results implied that SCAP was crucial in the control of the sterol metabolism and that our mouse line worked.

Inhibition of *Scap* expression and subsequent lipid synthesis in traditional primary astroglial culture did not show apparent alterations in conformational morphology or impact of cell growth. One of the possible limitations was the relatively low yields of GFAP positive cells in the culture, only around 25% in this approach. Primary cultures of astroglial cells grow rapidly in serum-containing medium, but compared with in vivo micro-environment, ambient presence of serum is not physiological. Moreover, by this traditional method, purification of mature astrocytes without contamination of other glial cells and precursor cells is difficult. As a result, we challenged a novel method of primary astrocyte culture by immunopanning. By using this method, purification of mature astrocytes becomes feasible²⁷. In fact, we compared these two methods of primary culture and found more than 90% of GFAP positive cells in the primary astrocyte culture by immunostaining. After 100 nM of 4-OH tamoxifen was given to inhibit the expression of *Scap* in Cre positive culture plate, we discovered that the number of surviving astrocytes decreased dramatically compared with that in Cre negative culture plate following the same time course. The ratio of GFAP positive cells was also decreased, compatible with the findings that GFAP-positive cells were the

main population affected by the tamoxifen induction. Comparison of mRNA profiles of remaining cells between both groups showed that expression of both *Scap* and *Gfap* significantly decreased. Because the sterol-regulatory genes such as *Srebf2*, *Hmgcr*, *Ldlr*, *Sqle*, and *Insig1* were all decreased, similarly to the results in traditional astroglial culture, we made the speculation that expression of *Scap* and subsequent sterol synthesis in primary astrocyte culture with serum-free medium was essential for their survival or cellular proliferation. This hypothesis may also explain the result that *Scap* mRNA decreased only 40 percent, not 100 percent in Cre positive primary culture with 4-OH tamoxifen by method of immunopanning, because GFAP positive cells in the plate also decreased in the ratio whereas GFAP negative cells, which were not supposed to be influenced by 4-OH tamoxifen, proliferated with time. Of course we could not totally rule out another possibility that inhibition of *Scap* expression might directly affect *Gfap* expression, however, our previous study presented that mice with homozygous knockout of *Scap* gene by nestin-Cre induced gliosis, which worked as the opposite direction that GFAP expression increased.

The finding that expression of SCAP was necessary for cell growth or survival seemed to be controversial with previous studies. Knockout of *Scap* in hepatocytes decreased synthesis of fatty acid and cholesterol, but it did not result in cell death or

apoptosis. Moreover, *Scap* knockout mice with constitutive *Gfap*-Cre which worked since embryonic stage did not show decreased ratio of astrocytes over neurons in hippocampus or cortex^{18,47}. To explain this contradiction, we speculate that hepatocytes incapable of synthesizing sterols by themselves may survive by uptake of ambient sterols or some other specific molecules from outer environments in the blood vessels or from adjacent tissues. Furthermore, because radial glial cells which had potential to transform into both neurons and astrocytes in the early development also expressed GFAP, *Scap* knockout in GFAP positive cells from the beginning of ontogeny would not only affect development of astrocytes but also that of neurons. Culture medium used in the method of immunopanning did not contain any serum or lipoproteins. Therefore, cell survival was dependent on the sterol synthesis by themselves. This presumption also matched up with the finding that no conformational or cellular changes were noted in traditional astroglial cells when *Scap* gene was knocked out, since there were abundant sterols in serum-containing medium. Cells may survive by uptake of sterol or some other specific molecules from the medium. To substantiate our hypothesis, we are considering further experiments to investigate the amount of cholesterol in primary astrocyte culture by fluorescent staining with filipin, a compound to combine with cholesterol specifically⁴⁸. Moreover, the molecular pathway needs to be clarified to

explain correlative cell death or apoptosis when sterol synthesis is inhibited by knockout of *Scap* gene.

By using the model of *hGFAP-CreERT2(Tg)::Scap flox* mice, we successfully knocked out the *Scap* gene in GFAP positive cells in adult mice. We discovered that induction of *Scap* deletion in astrocytes did not affect the brain structure, growth, body weight changes, food intake, insulin resistance, glucose tolerance or motor ability, whereas long-term memory of the GFAP-SCAP(-) mice was impaired as evidenced by passive avoidance test. In addition, the GFAP-SCAP(-) mice indicated improper stress responses and presented impulsiveness by the results of elevated plus maze and elevated platform test. In fact, previous studies also indicated that unbalanced sterol metabolism in the central nervous system led to changes of behavioral patterns. Mice with *Scap* heterozygous knockout with nestin-Cre was first reported with cognitive dysfunction combined with improper stress responses by behavioral tests²⁰. Furthermore, mice with *Scap* knockout with constitutive *Gfap*-Cre from the embryonic stage showed reduced anxiety with progressive motor deficits, dyskinesia and microcephaly, and high fat diet ameliorated the above symptoms except reduced anxiety, indicating that motor dysfunction and stress-related response may share different molecular pathways⁴⁷. Studies in humans had also suggested that membranous cholesterol in the central

nervous system was involved in major depression and suicidal behavior⁴⁹. Another study showed that it varied widely in cholesterol level and there was a significant decrease of cholesterol to phospholipid ratio in the brain in violent suicides compared to non-violent suicides by post-mortem autopsy⁵⁰. All the evidence point out the possibility that lipid metabolism in the central nervous system may have an impact on emotion, anxiety and impulsiveness. Therefore, in our study, GFAP-positive cells in the central nervous system may involve in the integration of drive impulse when various stressor existed. However, the molecular mechanisms or pathways explaining this phenomenon are still lacking and remain largely undiscovered.

GFAP-SCAP(-) mice in this study also lacked shortening of the interaction time to the same intruders according to the results of social recognition test. Because social interactions to the intruder mouse involve in mixed skills of stress response and memory, both impulsiveness and impairment of memory recall may be possible reasons to explain their poor social recognition ability compared with the control mice.

Several other possible mechanisms were considered. Some reports indicated that the hypothalamus-pituitary-adrenal gland (HPA) axis was important for the regulation of stress responses. Mice overproducing corticotrophin-releasing hormone (CRH) exhibited increased corticosteroid levels in serum and enhanced anxiety in behavioral

patterns. Mutant mice with disruption of glucocorticoid receptor gene in the central nervous system also indicated elevated concentrations of glucocorticoid in serum but an impaired behavioral response to stress and displayed reduced anxiety^{51, 52}. Based on these findings, we checked the relevant stress-related hormones such as corticosterone, epinephrine, ACTH and CRH of the diurnal rhythm in our mice, then also evaluated the responses of hormonal changes before and after the stressor such as fasting (considered as a chronic stressor) and 40 minutes period of restraint (considered as an acute stressor). However, there were no significant changes observed in GFAP-SCAP(-) mice compared with the control mice. Because the blood sampling from facial vein in mice was at least invasive, it was possible that small difference in the stress response might have been undetectable or masked by the procedures. Measuring corticosterone levels from the urine in both GFAP-SCAP(-) and control mice should be considered in the future. At the moment, we concluded that hormonal changes in our model might not explain the behavioral phenotypes.

Astrocytes have essential roles for maintaining the integrity of blood brain barrier. Regulation of VEGF- α and angiopoietin 1 (ANG-1) is an important factor to balance this homeostasis⁵³. Previous studies reported that astrocyte-derived IL-6, an inflammatory cytokine and its receptor alpha (IL-6RA) mediated anxiety, learning and

social behavior in mice^{54, 55}. By quantitative rt-PCR, we found that mRNA expression of IL-6 and IL-6RA was slightly elevated in Cre positive culture by method of immunopanning after knockout of SCAP by tamoxifen, though no statistical significance was reached. Either in the traditional astroglial culture or in the culture by immunopanning, there were no significant changes in the mRNA expression of VEGF- α and angiopoietin 1 (ANG-1) in Cre-positive cultures between with and without tamoxifen. Further investigation is required in the future.

Analyzing the lipid profiles in the brains of our animal model in vivo will be the next target, because understanding more about the flow and fluidity of lipid rafts when *Scap* was deficient in the astrocytes is the key to unravel the mechanisms of the phenotypes of the mice. In the previous study, cholesterol exposure caused activation of astrocytes, accelerating the production and processing of amyloid precursor protein⁵⁶. It will be helpful to check the differences of lipid rafts in certain areas of brains and the changes of amount of reactive oxygen species between GFAP-SCAP(-) mice and the control mice in the near future.

Besides that, we also assume the possibility of involvement of adult neurogenesis in the hippocampal dentate gyrus and subventricular as a potent mechanism. In the past, neurogenesis in rodents was generally considered to be halted in late postnatal

adulthood; however, recent evidence has revealed that adult neurogenesis occurs continually in subventricular zone of the lateral ventricle and the hippocampal dentate gyrus in the adult mammalian forebrain, and it can be related to stress responses^{57, 58}. Interestingly, the majority of these neural progenitor cells were later found to be GFAP-expressing cells⁵⁸. In fact, some evidence suggested that adult neurogenesis was implicated in the regulation of anxiety and depression. Neurogenesis-deficient mice showed increased anxiety and food avoidance in a novel environment⁵⁹. In our study, we also considered that administration of tamoxifen would result in *Scap* deficiency in GFAP positive cells, which consisted of not only astrocytes but also some GFAP positive neural progenitors in adult mice. Dysregulated sterol synthesis in these progenitor cells might cause the phenotype of improper stress responses and establishment of processes in long term memory. However, we have not corroborated this point of view experimentally. Further experiments are required to confirm this hypothesis.

Our previous paper raised the hypothesis that sterol synthesis in the astrocytes was important in stability of tripartite synapse and glial-neuron interaction. However, direct evidence of the impacts on neurons caused by deficiency of sterol synthesis in the adjacent astrocytes is yet to be indicated. We consider co-culture experiments of

astrocytes and neurons to make comparison by observing growth pattern of neurites and synapses after *Scap* was knocked out in the underlying astrocytes.

All knowledge we have in hand is that the dysfunctional regulation of SREBP/SCAP system in the whole brain in severe diabetic condition are based on the studies on mouse experiments. By now, there are no human studies in relation to diabetes and cholesterol metabolism in brains. Although the mouse we generated in this study is not a pathological animal model mimicking certain clinical conditions, by using this artificial approach, we expect that the function of SCAP in astrocytes can be clarified as a potent mechanism of cognitive dysfunction in diabetes.

In conclusion, Figure 19 indicates the summarized findings in this study, presenting hypothesis with some possible mechanisms involving sterol synthesis in GFAP positive cells to explain the phenotype. In primary astrocyte culture, deletion of *Scap* gene is supposed to cause defects in sterol synthesis. In the brain in vivo or in the environment with abundant ambient sterols in vitro, astrocytes incapable of synthesizing sterol themselves can survive and grow by uptake of sterol. However, without support of sterol from the outer environment, SCAP-deficient astrocytes are unable to proliferate or even survive for a long time. We speculate that induction of *Scap* deletion in GFAP positive cells may have impacts on the integrity and maturation of synapses to affect the

secretion of neurotransmitter, to change the pattern of adult neurogenesis, and to inhibit the active remodeling of neuron-to-neuron interactions in vivo. GFAP-SCAP(-) mice showed less anxiety, improper stress response compared with the control mice. Social interaction and consolidation of long term memory were impaired.

Understanding the alterations in lipid metabolism in the brain due to diabetes is crucial, because increased risk of cognitive impairment or other neurodegenerative diseases may be partly attributed to the change in lipid, which can be a treatable target. Once we could discover further clues for the link between lipid alteration in astrocytes impacting on neurons and the consequent change in behavioral patterns, they should have a great potential for finding a novel strategy to combat against the diabetes-related cognitive dysfunction and accompanying behavioral and psychological symptoms of dementia (BPSD), for cure or for prevention in advance.

VIII. Conflict of Interests

The author declares no Conflict of Interests.

IX. Acknowledgement

First of all, the author thanks Dr. Ryo Suzuki for his expertise in teaching and instructions to guide all the experiments. The author also thanks Drs. Ai Terai, Mikiko Haraguchi, Ryusuke Watanabe, Kuniko Saiki for their assistance to accomplish all behavioral studies and in vitro cell cultures. In addition, the author thanks Dr. Akiko Hayashi-Takagi (Center for Disease Biology and Integrative Medicine, Faculty of Medicine, The University of Tokyo) for teaching novel object recognition tests; Dr. Hotaka Fukushima (Department of Bioscience, Faculty of Applied Bioscience, Tokyo University of Agriculture) for valuable comments on passive avoidance tests and social recognition tests. Finally, the author sincerely appreciates Professor Takashi Kadowaki for his sound advice and continuous support to this project.

X. References

1. Neville, S. E. *et al.* Diabetes in Japan: a review of disease burden and approaches to treatment. *Diabetes Metab. Res. Rev.* **25**, 705-716 (2009).
2. Nathan, D. M. *et al.* Intensive diabetes treatment and cardiovascular disease in patients with type 1 diabetes. *N. Engl. J. Med.* **353**, 2643-2653 (2005).
3. Holman, R. R., Paul, S. K., Bethel, M. A., Matthews, D. R. & Neil, H. A. 10-Year Follow-Up of Intensive Glucose Control in Type 2 Diabetes. *N. Engl. J. Med.* **359**, 1577-1589 (2008).
4. Ohkubo, Y. *et al.* Intensive insulin therapy prevents the progression of diabetic microvascular complications in Japanese patients with non-insulin-dependent diabetes mellitus: a randomized prospective 6-year study. *Diabetes Res. Clin. Pract.* **28**, 103-117 (1995).
5. Ott, A. *et al.* Diabetes mellitus and the risk of dementia: The Rotterdam Study. *Neurology* **53**, 1937-1942 (1999).
6. Ohara, T. *et al.* Glucose tolerance status and risk of dementia in the community: the Hisayama study. *Neurology* **77**, 1126-1134 (2011).

7. Ninomiya, T. Diabetes mellitus and dementia. *Curr. Diab Rep.* **14**, 487-014-0487-z (2014).
8. Sims-Robinson, C., Kim, B., Rosko, A. & Feldman, E. L. How does diabetes accelerate Alzheimer disease pathology? *Nat. Rev. Neurol.* **6**, 551-559 (2010).
9. Bjorkhem, I. & Meaney, S. Brain cholesterol: long secret life behind a barrier. *Arterioscler. Thromb. Vasc. Biol.* **24**, 806-815 (2004).
10. Dietschy, J. M. & Turley, S. D. Thematic review series: brain Lipids. Cholesterol metabolism in the central nervous system during early development and in the mature animal. *J. Lipid Res.* **45**, 1375-1397 (2004).
11. Dietschy, J. M. & Turley, S. D. Cholesterol metabolism in the brain. *Curr. Opin. Lipidol.* **12**, 105-112 (2001).
12. Valenza, M. *et al.* Dysfunction of the cholesterol biosynthetic pathway in Huntington's disease. *J. Neurosci.* **25**, 9932-9939 (2005).
13. Jira, P. E. *et al.* Smith-Lemli-Opitz syndrome and the DHCR7 gene. *Ann. Hum. Genet.* **67**, 269-280 (2003).

14. Shobab, L. A., Hsiung, G. Y. & Feldman, H. H. Cholesterol in Alzheimer's disease. *Lancet Neurol.* **4**, 841-852 (2005).
15. Horton, J. D., Goldstein, J. L. & Brown, M. S. SREBPs: activators of the complete program of cholesterol and fatty acid synthesis in the liver. *J. Clin. Invest.* **109**, 1125-1131 (2002).
16. Sato, R. *et al.* Sterol-dependent transcriptional regulation of sterol regulatory element-binding protein-2. *J. Biol. Chem.* **271**, 26461-26464 (1996).
17. Amemiya-Kudo, M. *et al.* Promoter analysis of the mouse sterol regulatory element-binding protein-1c gene. *J. Biol. Chem.* **275**, 31078-31085 (2000).
18. Matsuda, M. *et al.* SREBP cleavage-activating protein (SCAP) is required for increased lipid synthesis in liver induced by cholesterol deprivation and insulin elevation. *Genes Dev.* **15**, 1206-1216 (2001).
19. Suzuki, R. *et al.* Diabetes and insulin in regulation of brain cholesterol metabolism. *Cell. Metab.* **12**, 567-579 (2010).

20. Suzuki, R., Ferris, H. A., Chee, M. J., Maratos-Flier, E. & Kahn, C. R. Reduction of the cholesterol sensor SCAP in the brains of mice causes impaired synaptic transmission and altered cognitive function. *PLoS Biol.* **11**, e1001532 (2013).
21. Pfrieger, F. W. & Ungerer, N. Cholesterol metabolism in neurons and astrocytes. *Prog. Lipid Res.* **50**, 357-371 (2011).
22. Kettenmann, H. & Verkhratsky, A. Neuroglia--living nerve glue. *Fortschr Neurol. Psychiatr.* **79**, 588-597 (2011).
23. Camargo, N., Smit, A. B. & Verheijen, M. H. SREBPs: SREBP function in glia-neuron interactions. *FEBS J.* **276**, 628-636 (2009).
24. Feil, R., Wagner, J., Metzger, D. & Chambon, P. Regulation of Cre recombinase activity by mutated estrogen receptor ligand-binding domains. *Biochem. Biophys. Res. Commun.* **237**, 752-757 (1997).
25. Hirrlinger, P. G., Scheller, A., Braun, C., Hirrlinger, J. & Kirchhoff, F. Temporal control of gene recombination in astrocytes by transgenic expression of the tamoxifen-inducible DNA recombinase variant CreERT2. *Glia* **54**, 11-20 (2006).

26. McCarthy, K. D. & de Vellis, J. Preparation of separate astroglial and oligodendroglial cell cultures from rat cerebral tissue. *J. Cell Biol.* **85**, 890-902 (1980).
27. Foo, L. C. *et al.* Development of a method for the purification and culture of rodent astrocytes. *Neuron* **71**, 799-811 (2011).
28. Miyata, S., Yamada, N., Hirano, S., Tanaka, S. & Kamei, J. Diabetes attenuates psychological stress-elicited 5-HT secretion in the prefrontal cortex but not in the amygdala of mice. *Brain Res.* **1147**, 233-239 (2007).
29. Surget, A. *et al.* Drug-dependent requirement of hippocampal neurogenesis in a model of depression and of antidepressant reversal. *Biol. Psychiatry* **64**, 293-301 (2008).
30. Walf, A. A. & Frye, C. A. The use of the elevated plus maze as an assay of anxiety-related behavior in rodents. *Nat. Protoc.* **2**, 322-328 (2007).
31. Steru, L., Chermat, R., Thierry, B. & Simon, P. The tail suspension test: a new method for screening antidepressants in mice. *Psychopharmacology (Berl)* **85**, 367-370 (1985).

32. Can, A. *et al.* The mouse forced swim test. *J. Vis. Exp.* (59):e3638. doi, e3638 (2012).
33. Sarnyai, Z. *et al.* Impaired hippocampal-dependent learning and functional abnormalities in the hippocampus in mice lacking serotonin(1A) receptors. *Proc. Natl. Acad. Sci. U. S. A.* **97**, 14731-14736 (2000).
34. Leger, M. *et al.* Object recognition test in mice. *Nat. Protoc.* **8**, 2531-2537 (2013).
35. Fukushima, H. *et al.* Upregulation of calcium/calmodulin-dependent protein kinase IV improves memory formation and rescues memory loss with aging. *J. Neurosci.* **28**, 9910-9919 (2008).
36. Karl, T., Pabst, R. & von Horsten, S. Behavioral phenotyping of mice in pharmacological and toxicological research. *Exp. Toxicol. Pathol.* **55**, 69-83 (2003).
37. Awazawa, M. *et al.* Deregulation of pancreas-specific oxidoreductin ERO1beta in the pathogenesis of diabetes mellitus. *Mol. Cell. Biol.* **34**, 1290-1299 (2014).
38. Ueki, K. *et al.* Increased insulin sensitivity in mice lacking p85beta subunit of phosphoinositide 3-kinase. *Proc. Natl. Acad. Sci. U. S. A.* **99**, 419-424 (2002).

39. Chong, A. C., Vogt, M. C., Hill, A. S., Bruning, J. C. & Zeltser, L. M. Central insulin signaling modulates hypothalamus-pituitary-adrenal axis responsiveness. *Mol. Metab.* **4**, 83-92 (2014).
40. Gutterer, J. M., Dringen, R., Hirrlinger, J. & Hamprecht, B. Purification of glutathione reductase from bovine brain, generation of an antiserum, and immunocytochemical localization of the enzyme in neural cells. *J. Neurochem.* **73**, 1422-1430 (1999).
41. Harno, E., Cottrell, E. C. & White, A. Metabolic pitfalls of CNS Cre-based technology. *Cell. Metab.* **18**, 21-28 (2013).
42. Reichenbach, A., Derouiche, A. & Kirchhoff, F. Morphology and dynamics of perisynaptic glia. *Brain Res. Rev.* **63**, 11-25 (2010).
43. Castagne, V., Moser, P., Roux, S. & Porsolt, R. D. Rodent models of depression: forced swim and tail suspension behavioral despair tests in rats and mice. *Curr. Protoc. Neurosci.* **Chapter 8**, Unit 8.10A (2011).
44. Ehlert, U., Gaab, J. & Heinrichs, M. Psychoneuroendocrinological contributions to the etiology of depression, posttraumatic stress disorder, and stress-related bodily

disorders: the role of the hypothalamus-pituitary-adrenal axis. *Biol. Psychol.* **57**, 141-152 (2001).

45. Kleinridders, A., Ferris, H. A., Cai, W. & Kahn, C. R. Insulin action in brain regulates systemic metabolism and brain function. *Diabetes* **63**, 2232-2243 (2014).

46. Brown, M. S. & Goldstein, J. L. Cholesterol feedback: from Schoenheimer's bottle to Scap's MELADL. *J. Lipid Res.* **50 Suppl**, S15-27 (2009).

47. Camargo, N. *et al.* High-fat diet ameliorates neurological deficits caused by defective astrocyte lipid metabolism. *FASEB J.* **26**, 4302-4315 (2012).

48. Gimpl, G. & Gehrig-Burger, K. Cholesterol reporter molecules. *Biosci. Rep.* **27**, 335-358 (2007).

49. Lalovic, A. *et al.* Cholesterol content in brains of suicide completers. *Int. J. Neuropsychopharmacol.* **10**, 159-166 (2007).

50. Freemantle, E., Mechawar, N. & Turecki, G. Cholesterol and phospholipids in frontal cortex and synaptosomes of suicide completers: relationship with endosomal lipid trafficking genes. *J. Psychiatr. Res.* **47**, 272-279 (2013).

51. Tronche, F. *et al.* Disruption of the glucocorticoid receptor gene in the nervous system results in reduced anxiety. *Nat. Genet.* **23**, 99-103 (1999).
52. Stenzel-Poore, M. P., Heinrichs, S. C., Rivest, S., Koob, G. F. & Vale, W. W. Overproduction of corticotropin-releasing factor in transgenic mice: a genetic model of anxiogenic behavior. *J. Neurosci.* **14**, 2579-2584 (1994).
53. Shen, F. *et al.* Coexpression of angiopoietin-1 with VEGF increases the structural integrity of the blood-brain barrier and reduces atrophy volume. *J. Cereb. Blood Flow Metab.* **31**, 2343-2351 (2011).
54. Quintana, A. *et al.* Astrocyte-specific deficiency of interleukin-6 and its receptor reveal specific roles in survival, body weight and behavior. *Brain Behav. Immun.* **27**, 162-173 (2013).
55. Erta, M., Giralt, M., Esposito, F. L., Fernandez-Gayol, O. & Hidalgo, J. Astrocytic IL-6 mediates locomotor activity, exploration, anxiety, learning and social behavior. *Horm. Behav.* **73**, 64-74 (2015).
56. Avila-Munoz, E. & Arias, C. Cholesterol-induced astrocyte activation is associated with increased amyloid precursor protein expression and processing. *Glia* (2015).

57. Mirescu, C. & Gould, E. Stress and adult neurogenesis. *Hippocampus* **16**, 233-238 (2006).

58. Garcia, A. D., Doan, N. B., Imura, T., Bush, T. G. & Sofroniew, M. V. GFAP-expressing progenitors are the principal source of constitutive neurogenesis in adult mouse forebrain. *Nat. Neurosci.* **7**, 1233-1241 (2004).

59. Snyder, J. S., Soumier, A., Brewer, M., Pickel, J. & Cameron, H. A. Adult hippocampal neurogenesis buffers stress responses and depressive behaviour. *Nature* **476**, 458-461 (2011).

XI. Figures

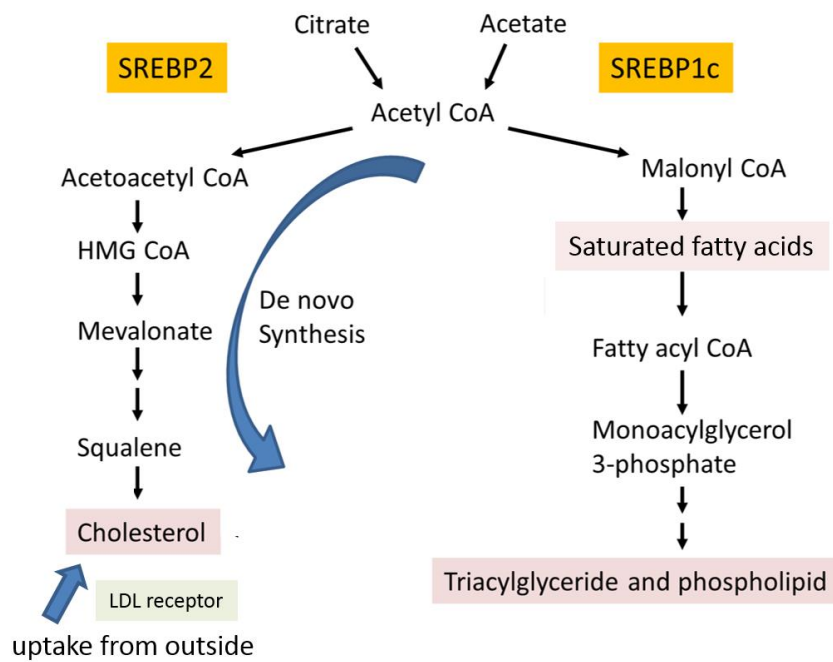


Fig. 1 The SREBP-dependent pathways for synthesizing cholesterol, fatty acids, and triglyceride. Both pathways start from the same molecule, acetyl-CoA. SREBP1c preferentially activates genes of fatty acid and triglyceride synthesis, whereas SREBP2 activates genes for cholesterol synthesis. LDL receptor mediates the uptake of cholesterol from the outer environment. Modified from reference 15.

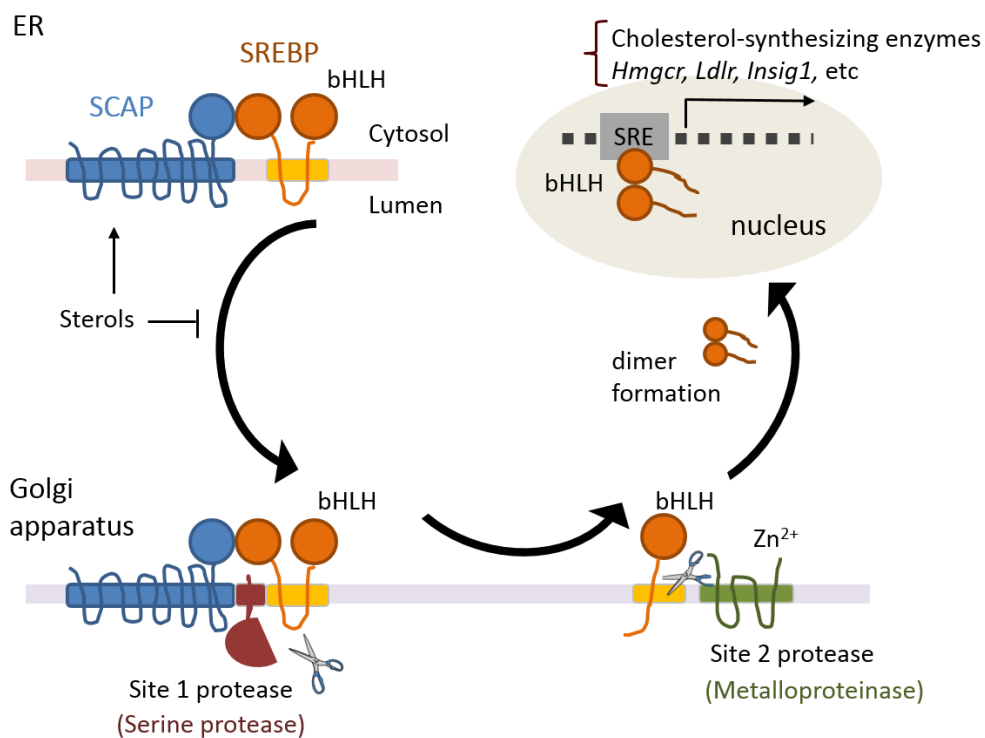


Fig. 2 A simplified model for regulation of cholesterol synthesis by sterol response element binding proteins (SREBPs) and SREBP-cleavage activating protein (SCAP). Precursor forms of SREBP are localized at the endoplasmic reticulum (ER) as a complex bound to SCAP. When sterols levels are low, SREBP:SCAP complex is transported from the ER to the Golgi apparatus by the escort of SCAP. In the Golgi apparatus, SREBP becomes activated by two proteases to be released into cytoplasm to form dimer. The dimer finally acts directly on SRE (sterol response element) in the enhancer/promoter regions of target genes related with cholesterol and fatty acid synthesis in the nucleus. Adapted from reference 15. bHLH: basic helix-loop-helix domain.

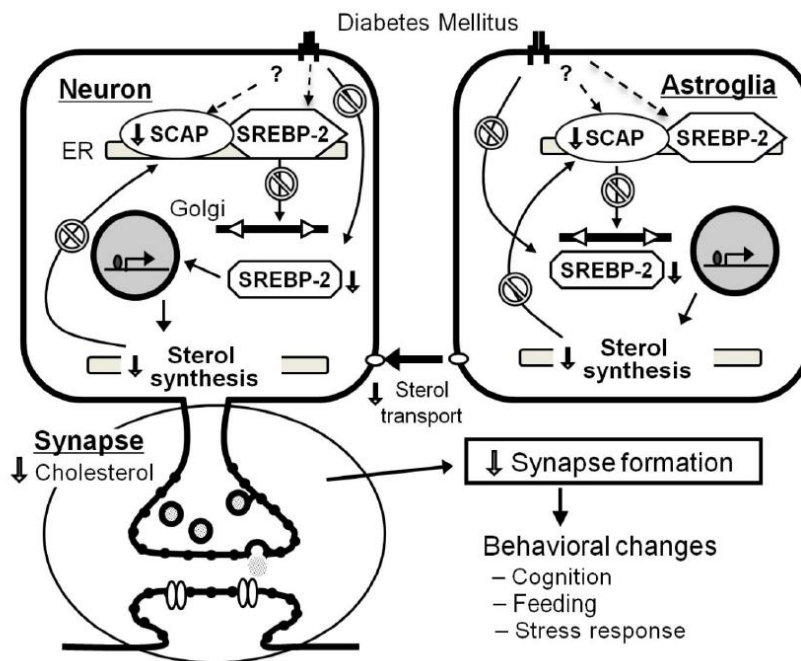


Fig. 3 One of the hypotheses for explaining the relationship between diabetes and behavioral changes including cognitive dysfunction and stress responses. Insufficient insulin action impairs activation of SREBP2 and hyperglycemia leads to degradation of SCAP in the central nervous system. Both changes result in the decreased amount of sterols in synaptosomes. Decreased sterol synthesis in synapses would cause structural and functional impairment, both of which are supposed to affect behavioral changes. Adapted from reference 20.

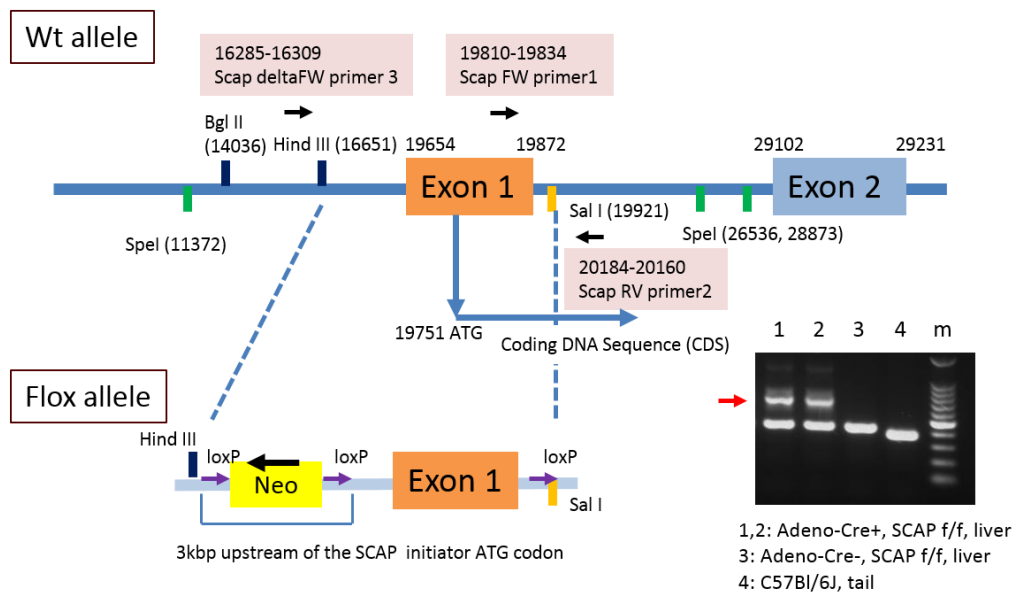


Fig. 4 Maps of wide-type allele and flox allele of mouse *Scap* gene, and the location of self-designed primers. Excision of the sequences between the loxP sites by the Cre recombinase deletes 3 kb of DNA sequence including exon 1. This genetic recombination reduces distance between annealing sites of primer 2 and primer 3, enabling to amplify the DNA fragment. As a result, a new band (knockout band, the red arrow) was detected when Cre recombinase was activated. Liver samples from *Scap* flox mice after injection of adenovirus vector expressing Cre recombinase were used as positive controls.

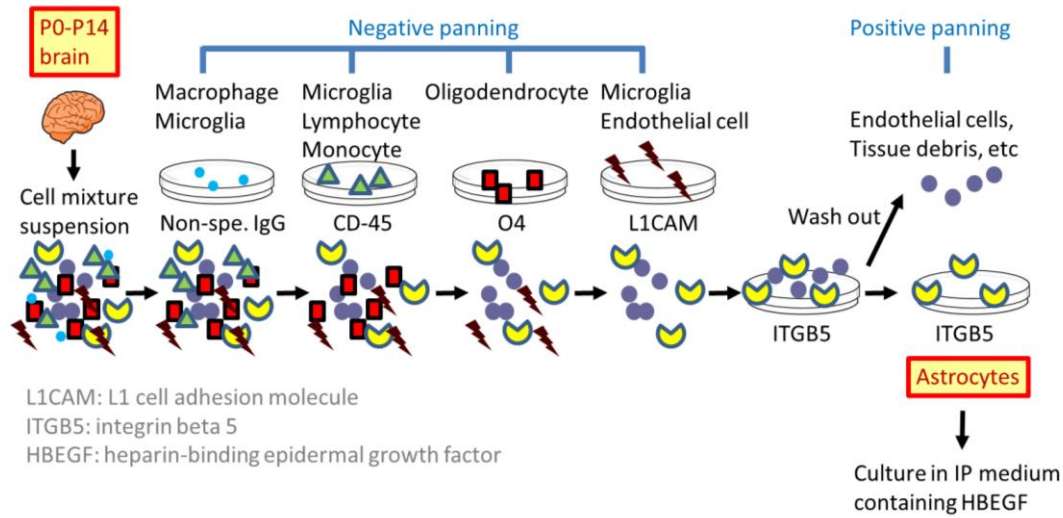


Fig. 5 The immunopanning (IP) method for purification of astrocyte. By utilizing specific antigen-antibody interaction, macrophages, lymphocytes, oligodendrocytes, and microglia were initially removed as negative selections. Next, astrocytes were trapped on the plate coated with antibody against astrocyte-specific surface antigen ITGB5 as positive selections. Finally astrocytes were collected and cultured in IP medium containing specific vascular trophic factors HBEGF instead of adding serum. Adapted from reference 25.

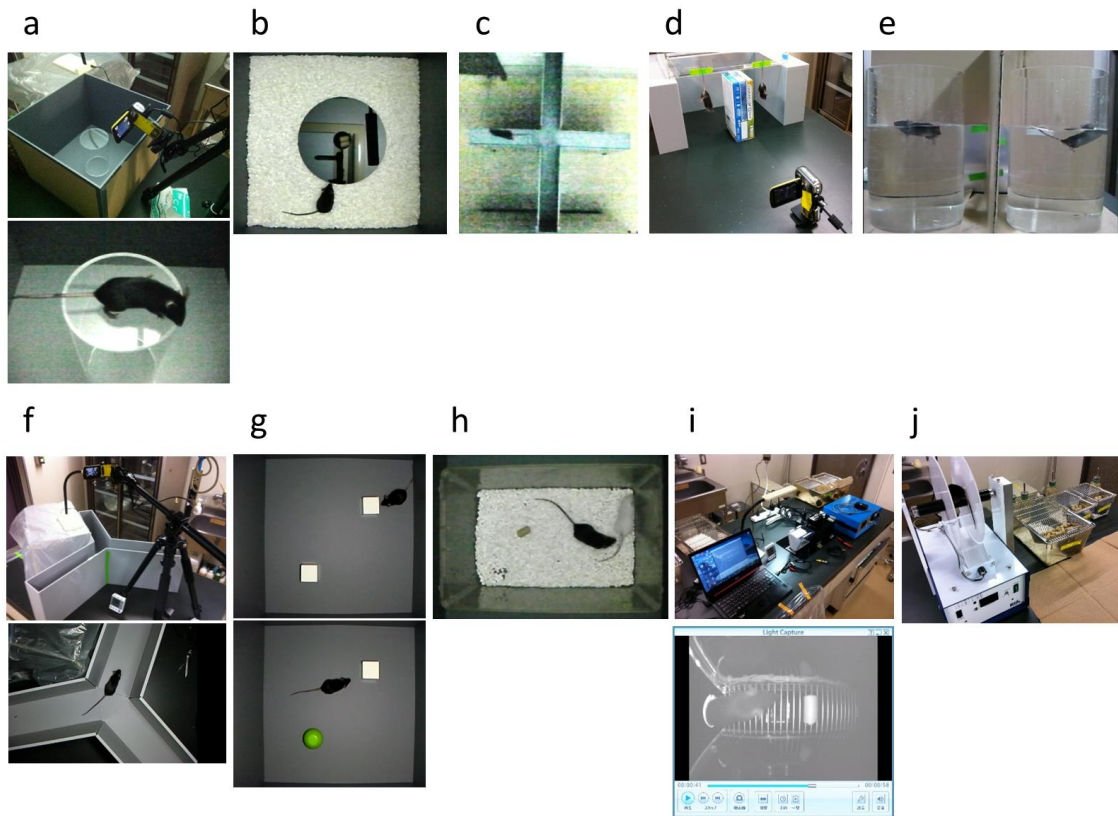


Fig. 6 Behavioral experiments performed in this study. See detailed description of each test in the section of ‘Materials and Methods’. a: elevated open-platform test. b: novelty suppressed feeding. c: elevated plus maze test. d: tail suspension test. e: forced swim test. f: Y maze. g: novel object recognition test. h: social recognition test. i: passive avoidance test. j: rotarod. Detailed timing for experiments is listed as follows: elevated open-platform test at 9-10 weeks of age; Y maze at 10 weeks of age; novelty suppressed feeding at 10-11 weeks of age; novel object recognition test at 11 weeks of age; rotarod at 11-12 weeks of age; tail suspension test at 12-13 weeks of age; social recognition test at 13-14 weeks of age; forced swim test at 13-15 weeks of age; elevated plus maze test at 14-15 weeks of age; passive avoidance test at 14-16 weeks of age.

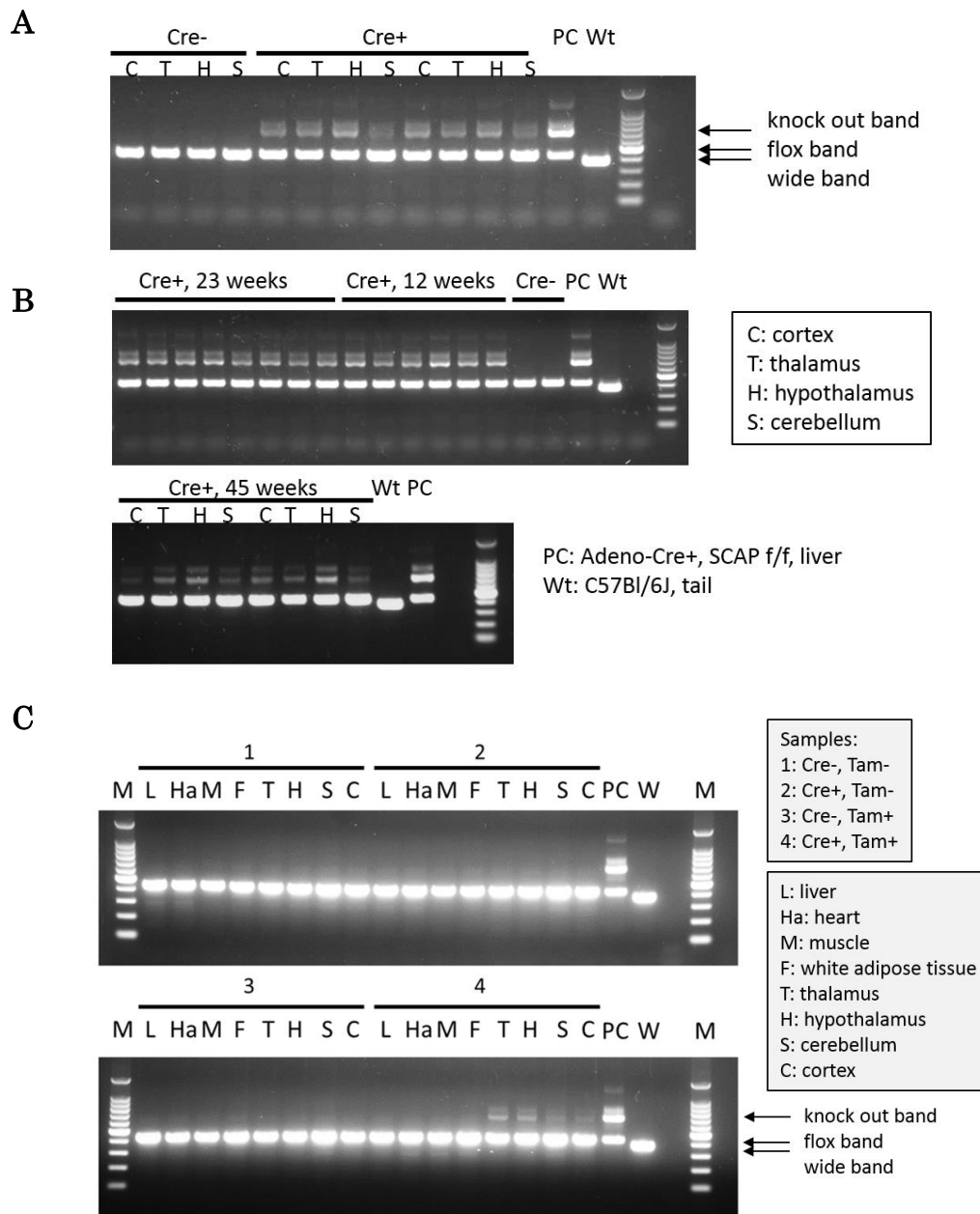


Fig. 7 Generation of *hGFAP-CreERT2(Tg)::Scap flox* mice. Mice received tamoxifen administration (2.0 mg/day for consecutive 8 days) at 8 weeks of age if given. A: After tamoxifen administration, knockout bands were detected in the cortex, thalamus, hypothalamus and cerebellum of Cre positive mice but not in those of Cre negative mice. B: After tamoxifen administration, the knockout bands were confirmed in Cre positive mice at 12 weeks of age and persisted at 45 weeks of age. C: there were no knockout bands in the other organs except brain in Cre positive mice after tamoxifen induction. Mice in A were sacrifice at 23 weeks of age; mice in C were sacrificed at 56 weeks of age.

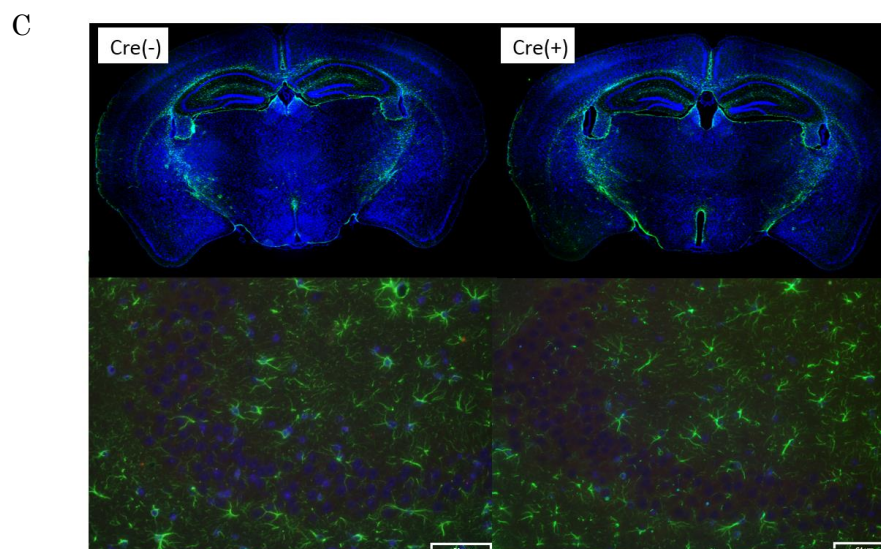
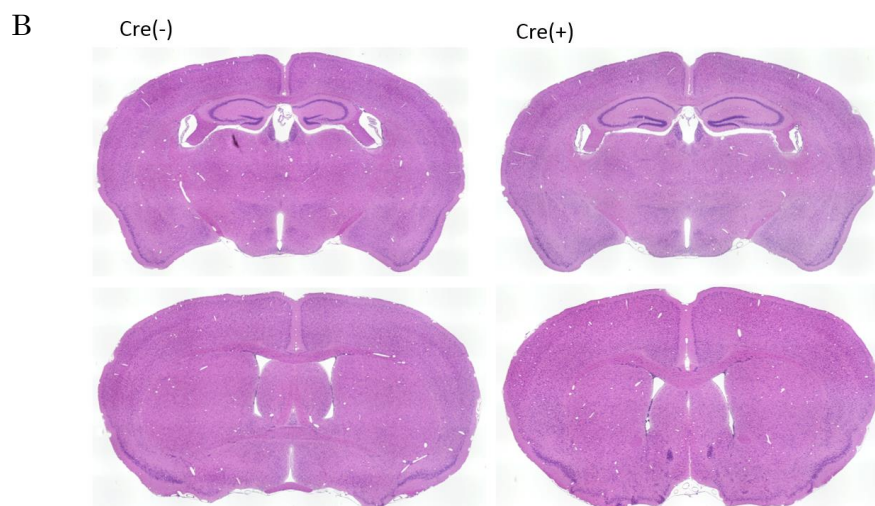
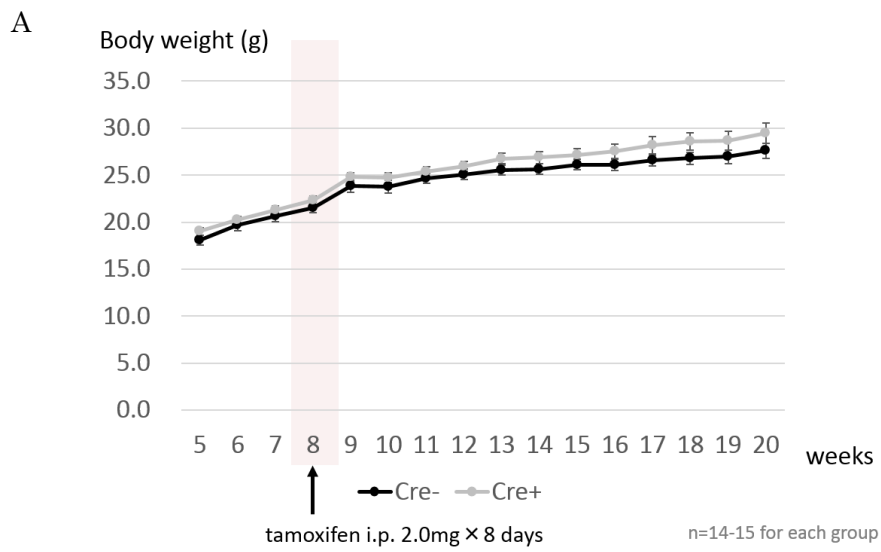


Fig. 8 Body weight changes and brain slices in *hGFAP-CreERT2(Tg)::Scap flox* mice. Tamoxifen was injected intraperitoneally (i.p.) at 8 weeks of age. A: Growth curves

from 5 weeks to 20 weeks of age. There were no significant differences in body weight between Cre positive and Cre negative mice before and after tamoxifen treatment. n=14-15 in each group. B: H&E staining of brain slices from mice at 12 weeks of age. No apparent differences were found in brain size, hippocampal atrophy, or ventricular enlargement between these two groups. Upper half: slices including hippocampal regions. Lower half: slices including paraventricular areas. C: GFAP immunostaining of brain slices from mice at 12 weeks of age. No apparent changes in the number of GFAP-positive cells between both groups. Upper half: slices including hippocampal regions. Lower half: CA3 areas in hippocampus. Green: GFAP. Blue: Hoechst staining. Bar equals 60 μ M in length.

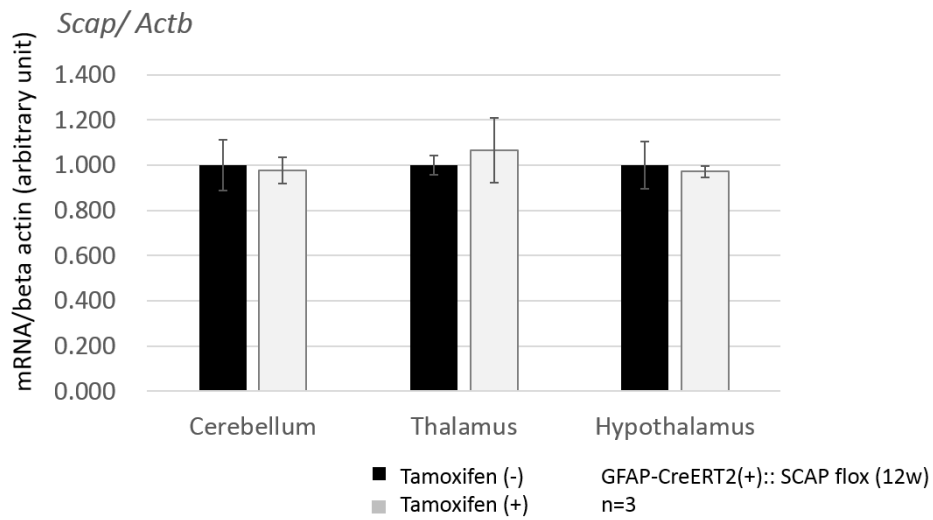


Fig. 9 Transcriptional expression of *Scap* in Cre positive mice with and without tamoxifen administration. Expression of *Scap* mRNA did not differ in the cerebellum, thalamus and hypothalamus of Cre positive mice before and after tamoxifen administration. Tamoxifen administration was performed at 8 weeks of age; samples were collected at 12 weeks of age. Beta actin was used as internal control. n=3 in each group.

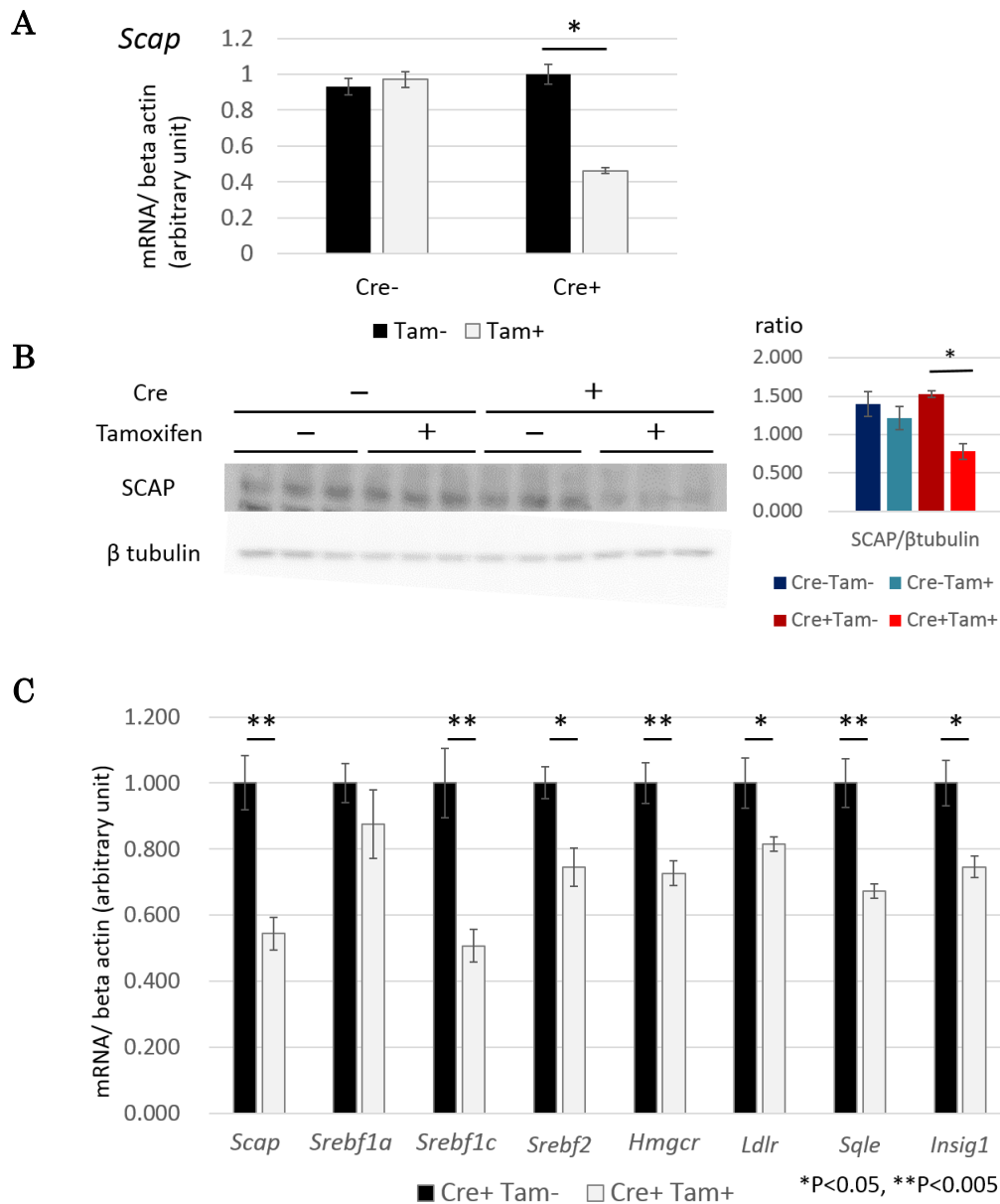


Fig. 10 Expression of *Scap* and its downstream genes from traditional astroglial culture. A: Significant decrease in mRNA expression of *Scap* was confirmed in Cre positive astroglial cultures after tamoxifen treatment. n=6 in each group B: Protein level of SCAP was also decreased in Cre positive astroglial cultures after tamoxifen treatment. Densitometry of western blotting is indicated at the right. n=3 in each group C: Transcriptional expression of *Srebf1c*, *Srebf2*, *Hmgcr*, *Ldlr*, *Sqle* and *Insig1* were decreased in Cre positive astroglial cultures after tamoxifen induction. No significant change in transcriptional expression of *Srebf1a* was noted. Beta actin was used as internal control. n=6 in each group. *P<0.05, and **P<0.005.

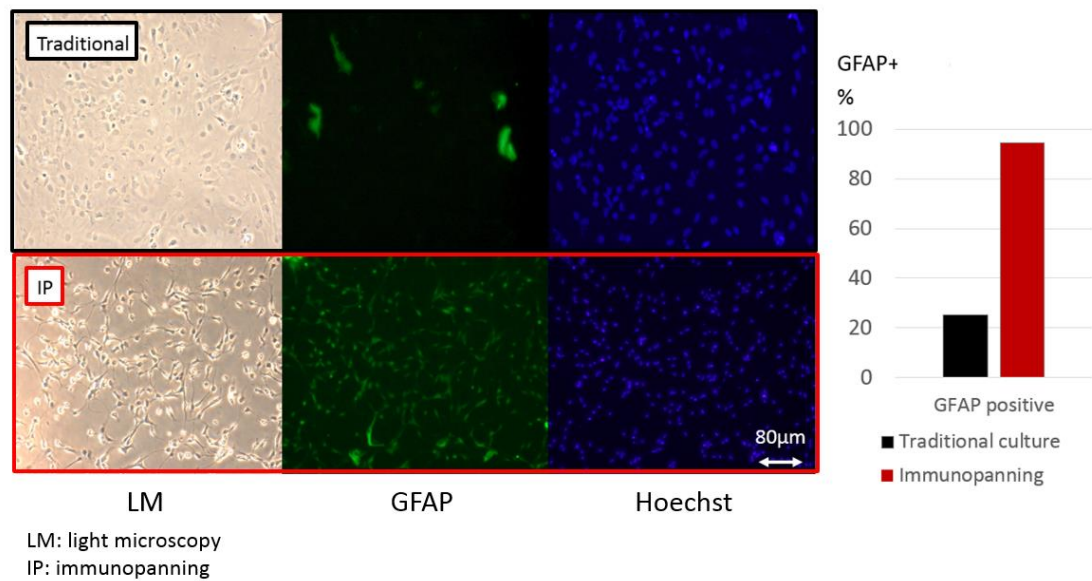


Fig. 11 Comparison between traditional astroglial culture (black frame) and primary astrocyte culture by method of immunopanning (red frame). By immunopanning, the ratio of GFAP positive cells increased dramatically and process-like microstructures became apparent. Morphology of the cells was fibroblast-like, and less than 25% were GFAP-positive by traditional astroglial culture. Counterstaining for all cell nuclei with Hoechst reagent.

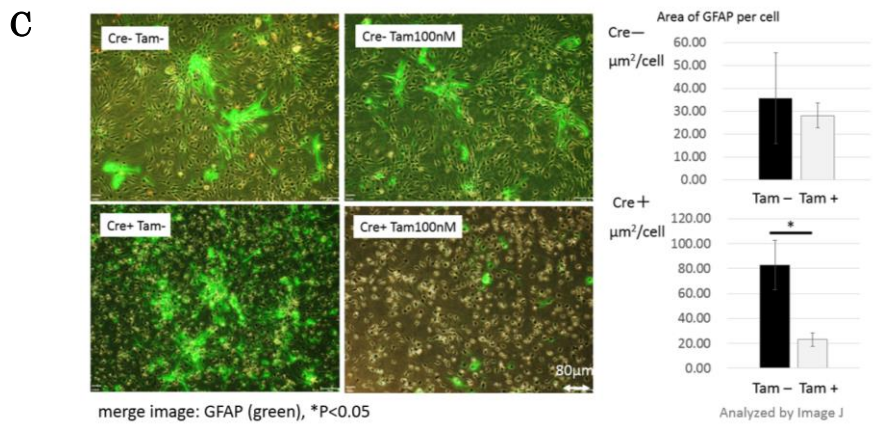
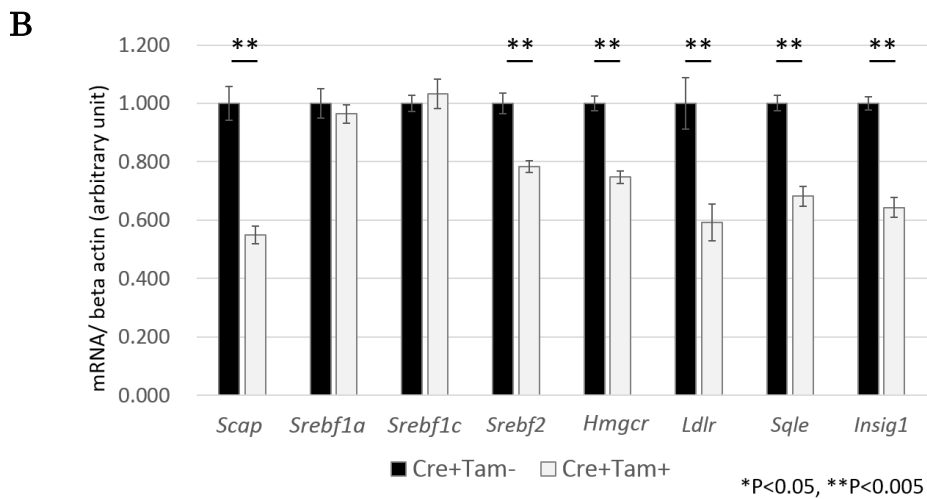
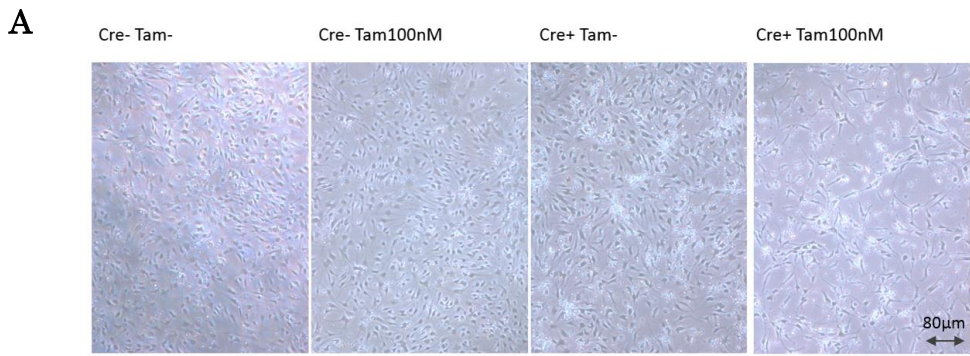


Fig. 12 Impaired growth or survival of GFAP positive cells in Cre positive astrocyte

culture after tamoxifen treatment. A: Under light microscopy, the number of surviving cells in Cre positive cell culture after tamoxifen treatment decreased significantly compared with the other three groups. B: Expression of *Scap* and its downstream genes from primary astrocyte by method of immunopanning were similar to the results from traditional astroglial culture. Cholesterol-related genes such as *Srebf2*, *Hmgcr*, *Ldlr*, *Sqle* and *Insig1* were all decreased when genetic recombination of *Scap* was induced by tamoxifen. n= 6 for each group. Beta actin was used as internal control. C: By immunostaining, GFAP-positive cells decreased in Cre positive group after tamoxifen induction. Both mRNA expression levels of *Scap* and *Gfap* were reduced. Calculation of GFAP area was performed and analyzed by ImageJ software. n=3 for each group.

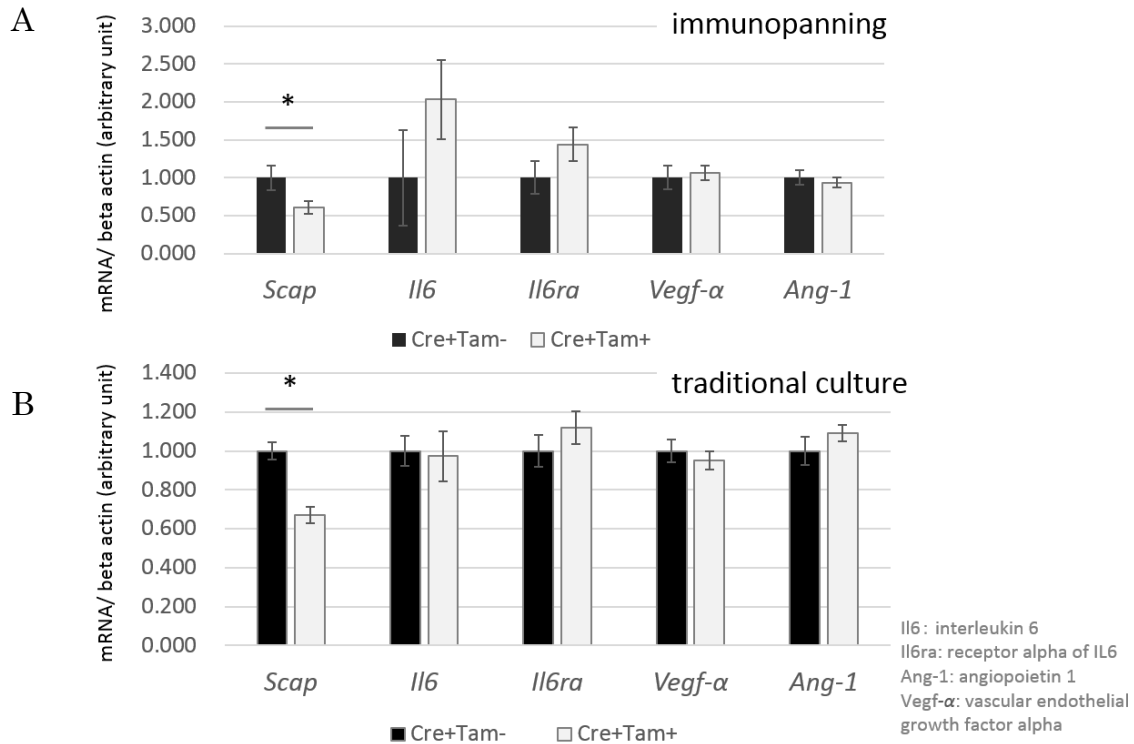


Fig. 13 mRNA expression of interleukin 6 (IL-6), interleukin 6 receptor alpha (IL6RA), VEGF- α and ANG-1 in primary astroglial culture and in primary astrocyte culture by immunopanning. A: mRNA expression of interleukin 6 (IL-6) and IL-6 receptor alpha (IL-6RA) seemed to be elevated in Cre positive primary astrocyte culture by method of immunopanning after conditional knockout of *Scap* by tamoxifen, though no significance was reached. B: No significant differences in mRNA expression of IL-6, IL6RA, VEGF-A and ANG-1 in traditional astroglial culture. Beta actin was used as internal control. n=6 for each group. * P<0.05.

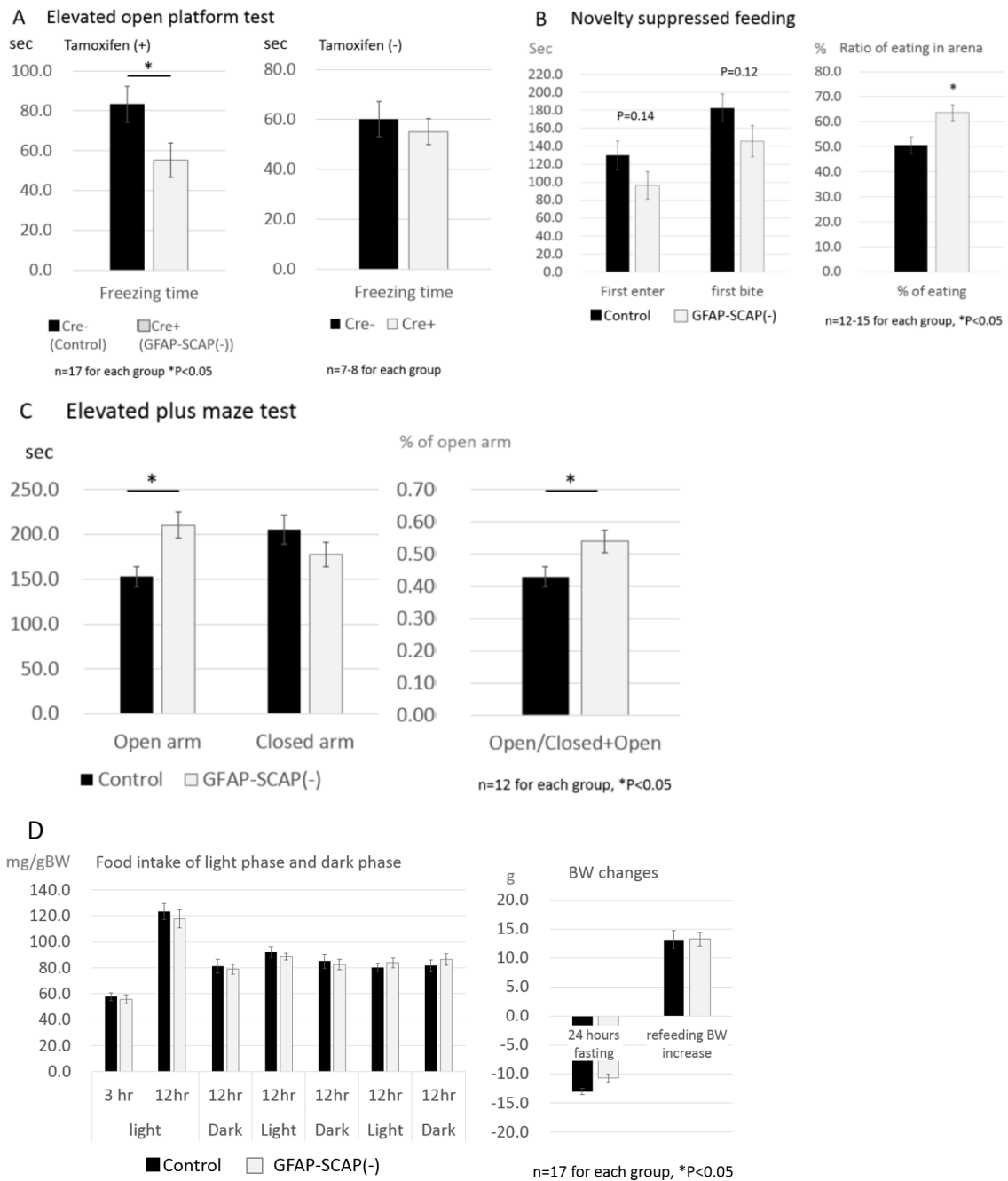


Fig. 14 Improper stress response was noted in the hGFAP-Cre-positive *Scap* flox mice after tamoxifen intraperitoneal injection (represented as GFAP-SCAP(-) below) compared with the control group (GFAP-Cre-negative *Scap* flox mice after tamoxifen injection). A: In elevated open-platform test, less freezing time was found in GFAP-SCAP(-) mice compared to the control mice but no differences if tamoxifen was not applied. B: GFAP-SCAP(-) mice showed shorter duration to enter the arena to start eating than the control, though no statistical significance was reached. However, time ratio of eating in arena was significantly higher in GFAP-SCAP(-) group. C: In elevated

plus maze test, GFAP-SCAP(-) mice tended to explore open arms more compared with the control mice. D: There was no differences in food intake between these two groups for continuous 72 hours monitoring after 24 hour fasting. No differences in body weight changes were found between the two groups, either in fasted or refed (for 72 hours) state. * $P < 0.05$. Number of the mice used for each group is described in the figure above.

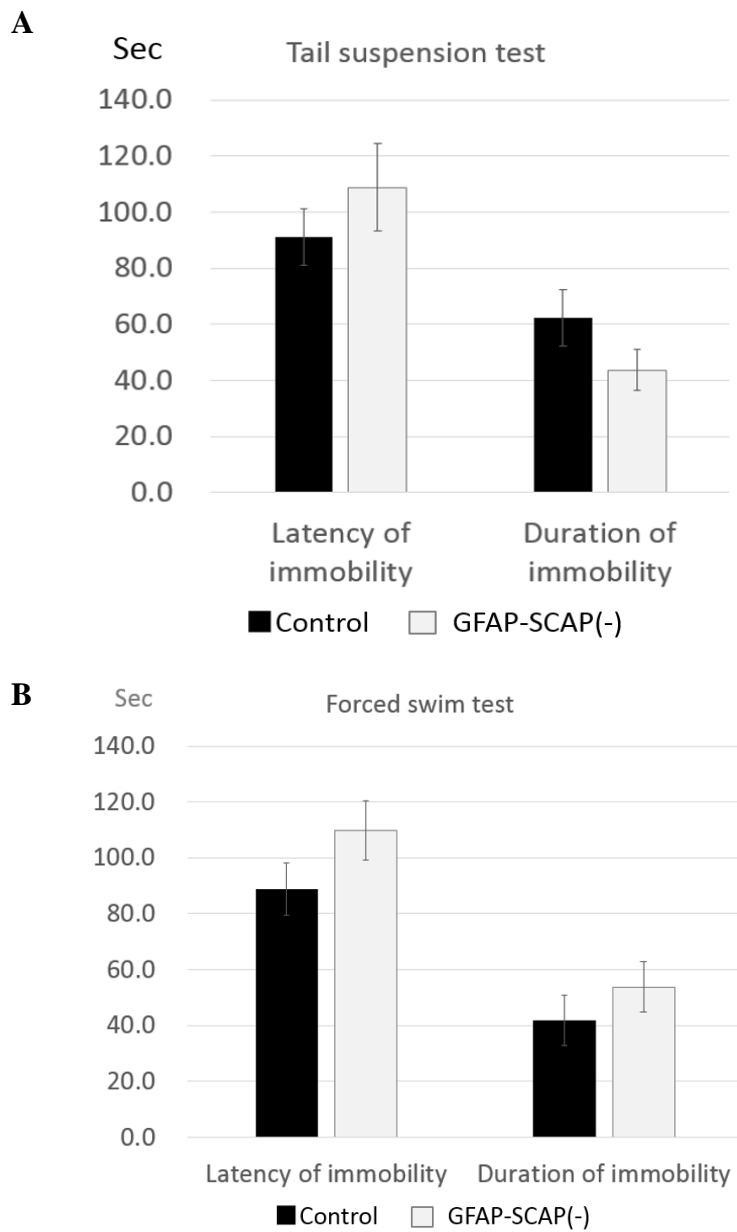


Fig. 15 Behavioral tests for evaluation of depressive status. No significant differences were noted between GFAP-SCAP(-) mice and the control mice in either A: tail suspension test or B: forced swim test. n= 17 in each group.

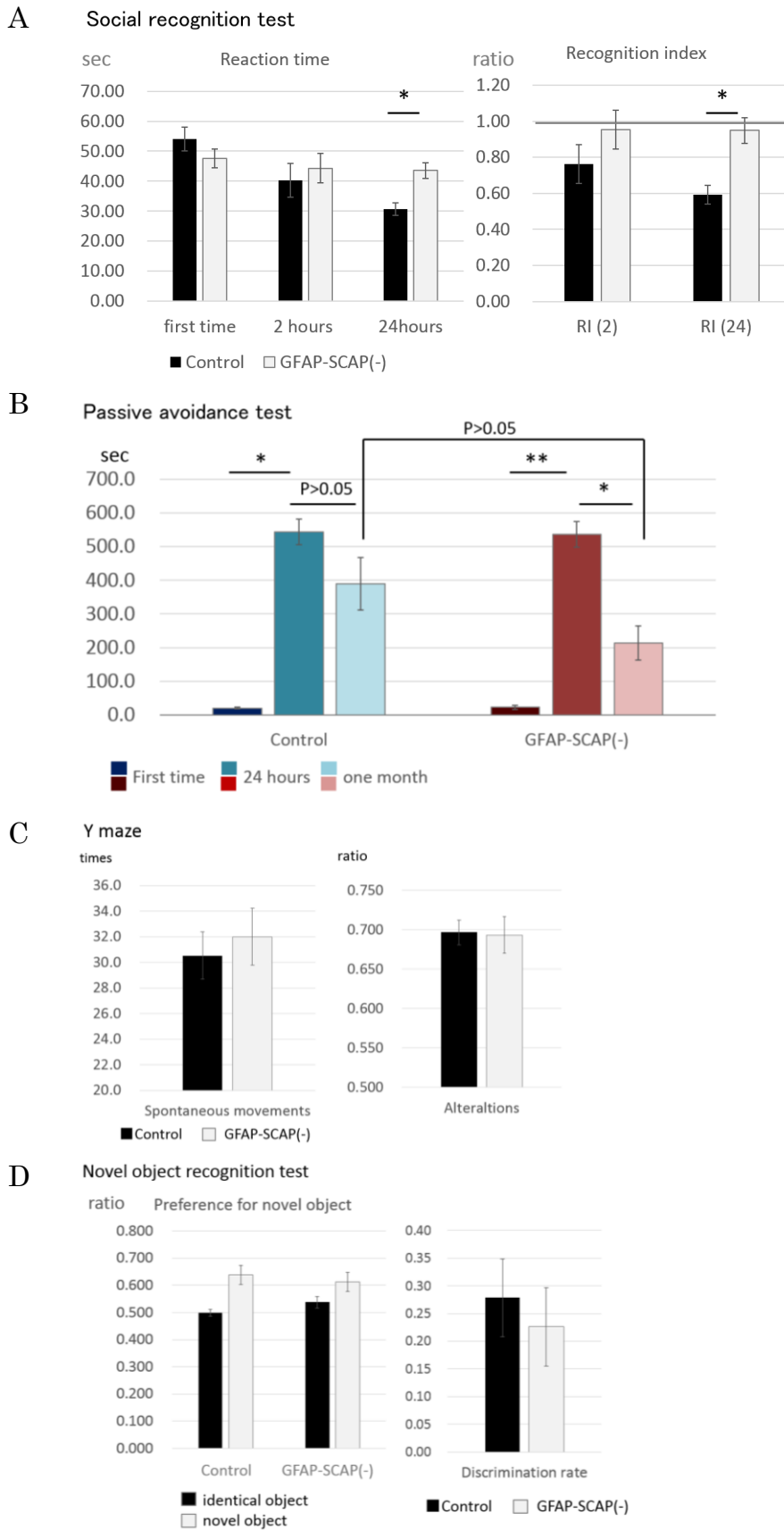


Fig. 16 GFAP-SCAP(-) mice showed impairment in consolidation of long-term memory

and improper social responses, but not in short-term memory or spatial learning. A: In social recognition test, the control mice became acclimated to the invader in progression, spending less time for approaching gradually. However, GFAP-SCAP(-) mice did not showed this tendency and spent similar time at the first visit, after 2 hours, and after 24 hours. $RI(2)$ = interaction time 2 hours after over that of first time. $RI(24)$ = interaction time 24 hours after over that of first time. B: Impaired consolidation of long-term memory was noted in GFAP-SCAP(-) mice by passive avoidance test, as less time spent to re-enter the dark chamber where electric shock was given one month ago. C: In Y maze, total numbers of entering arms and alterations were similar in both groups. D: In NORT, both groups of GFAP-SCAP(-) and the control mice showed more interests and spent much exploration time to the novel object than the identical one but no statistical differences between the two groups. Discrimination rate= (approaching time to novel object – that to identical object) / (approaching time to novel object + that to identical object). * $P < 0.05$, ** $P < 0.01$. For NORT, social recognition test and passive avoidance test, $n = 10-12$ in each group. For Y maze, $n = 17$ in each group.

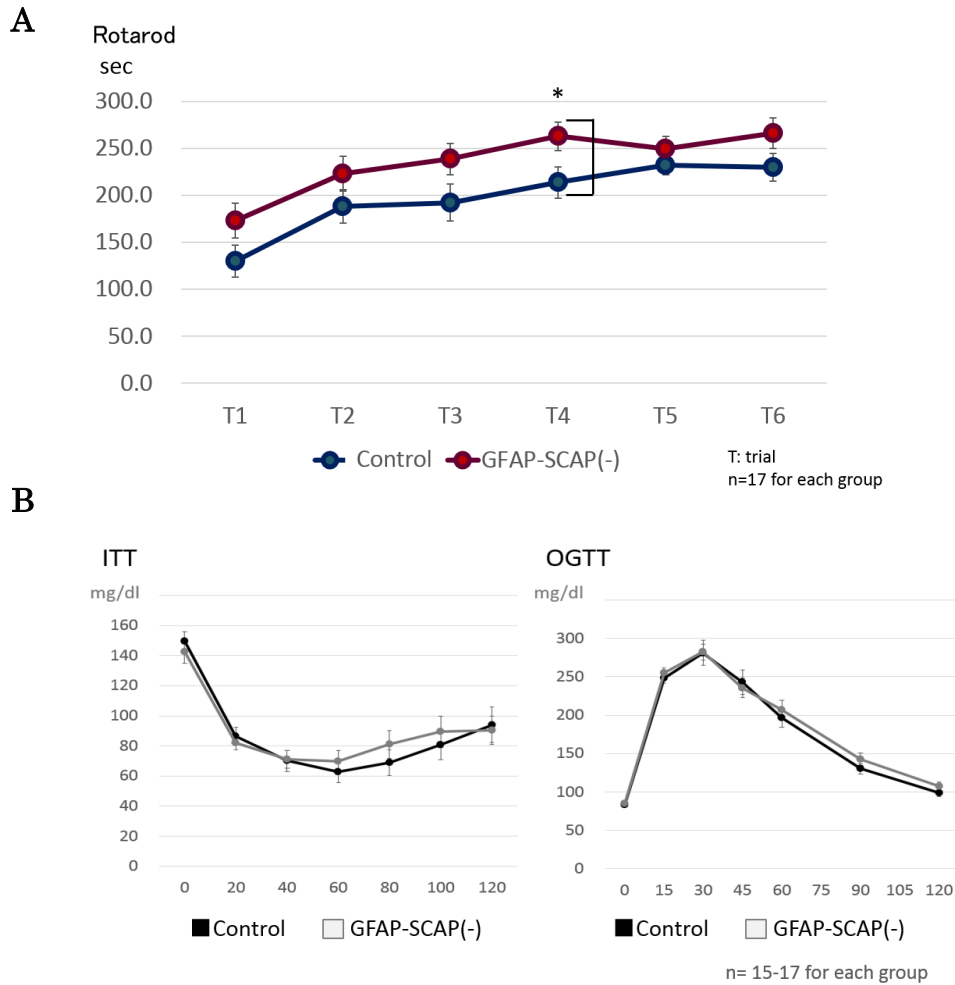


Fig. 17 A: GFAP-SCAP(-) mice did not show defects in co-ordination, balance or motor learning as evidenced by rotarod compared with the control group. GFAP-SCAP(-) mice even showed better running ability in the fourth trial compared with the control mice. Both groups showed better co-ordination and motor ability since the third trial compared with the first trial. B: No differences were found in insulin sensitivity by insulin tolerance test (ITT) or glucose tolerance by oral glucose tolerance test (OGTT) between GFAP-SCAP(-) and the control mice when fed by normal chow. For rotarod, ITT, and OGTT, n=15-17 in each group.

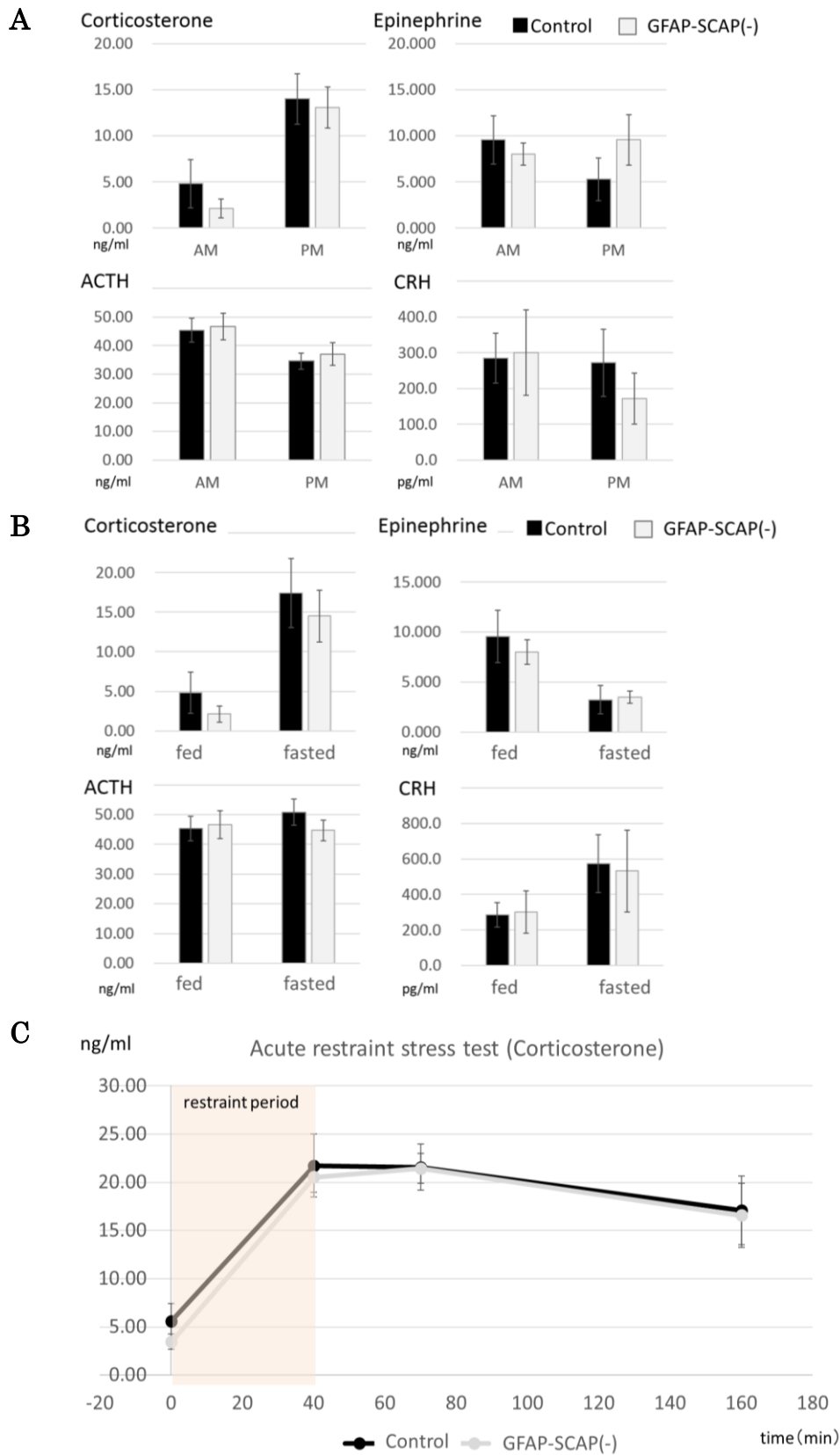


Fig. 18 Evaluation of stress-related hormones in hypothalamus-pituitary adrenal axis and responses of which after a chronic and an acute stressor. A: Diurnal rhythm of stress

related hormones. B: Alterations of stress related hormones under fed state with an ad libitum standard mouse chow and fasted state for 12 hours. No differences in corticosterone, epinephrine, ACTH or CRH levels were shown between GFAP-SCAP(-) mice and the control mice. Blood samples were taken in 9 AM. C: Evaluation of acute stress responses against restraint for 40 minutes revealed no significant differences in serum corticosterone between GFAP-SCAP(-) and the control mice. n=9-10 for each group.

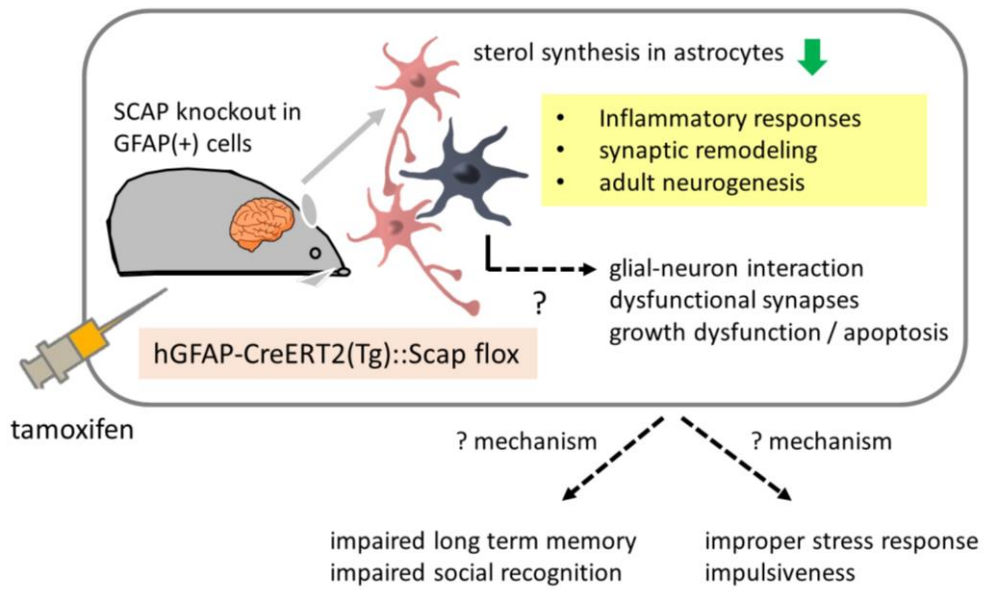


Fig. 19 Possible physiological function of SCAP in astrocytes. SCAP expression in astrocytes is at least partially responsible for lipid metabolism in the central nervous system. Inhibition of *Scap* expression by genetic knockout in astrocytes may affect the glial-neuron interaction, adult neurogenesis and break the stability of synapse via several pathways. According to this study, GFAP-SCAP(-) mice showed impaired long term memory and improper stress responses, yet mechanisms were still required to be elucidated.